GIANTLEAP

DELIVERABLE D5.3

PUBLIC

Results of experiments on BoP components

Peter Eckert (Bosch Engineering GmbH)
Quality Assurance: Frano Barbir (FESB)

GIANTLEAP

Project acronym: GIANTLEAP

Project title: Giantleap Improves Automation of Non-polluting Transportation with Lifetime Extension of Automotive PEM fuel cells

Project number: 700101

Document date: December 12, 2018

Due date: October 31, 2017

Keywords: balance of plant, BoP, ageing, durability, air compressor, humidifier, endurance testing

Abstract: In order to evaluate and extend the lifetime of automotive PEM fuel cell systems, durability and performance losses of the balance of plant (BoP) components play a major role. BEG had the responsibility within the Giantleap project to analyze the lifetime degradation of the main BoP components and deliver measurement data accordingly. Focus lay on the cathode path components, air compressor and humidifier. For both, one sample was dismantled, analyzed and the ageing mechanisms identified. From this knowledge, a test bench set-up and according test cycle was developed. A 500-hour endurance run produced measurement data for further evaluation and design of operation strategies and layout criteria. This data now is available to the other project partners in the project e-room. The endurance test delivered the proof that the system designed for Giantleap is fit to at least perform during the demonstration period. At the same time, considerable weaknesses of the components became evident. Over the duration of the tests performed, the humidifier lost about 50% of its calculated efficiency, which leaves room for further investigation and verification. The performance of the compressor remained stable through the whole endurance run with one capital failure due to an inappropriate operation point. Nevertheless, the subliminal danger of contamination by spilled traction oil remains and leaves the opportunity for oil-free bearing technologies open.

Revision History

Date	Description	Author
Nov 27, 2018	Draft Version 0.1	Peter Eckert
Dec 5, 2018	V 0.2: Implement internal corrections	Peter Eckert
Dec 12, 2018	Final version, typographical adjustments	Federico Zenith

GIANTLEAP

Table of Contents

1 Introduction

1.1 Document overview

The objective for the work package 5 is defined in the Giantleap proposal as follows:

"WP5: Fuel Cell Systems will integrate the full-size stacks together with BoP components into a full-fledged FC system, which will then be integrated further in a range extender for battery buses." (1)

WP5.3 includes the selection and evaluation of all BoP components for the fuel cell system with special consideration of cost and durability. This also includes conduction of experiments to evaluate the behavior of the must cost intensive components over lifetime.

1.2 Background and project context

Within WP5 BEG selected and purchased all BoP components to integrate the full size stacks provided by ElringKlinger through WP4 into a complete fuel cell system. After conduction a factory acceptance test, the full system will be provided to VDL for integration into a REEV electric bus.

System design, selection of BoP components and control strategies will consider the results of earlier research.

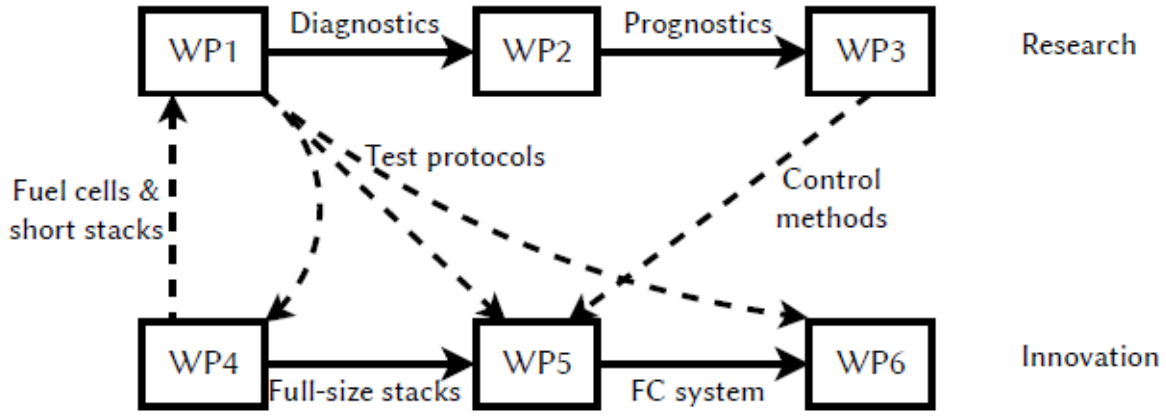

Fig. 1: Interaction of the different work packages within Giantleap project (1)

As mentioned earlier in D5.2 report, the hydrogen subsystem was mainly defined by ElringKlinger (integrated anode loop) and VDL (hydrogen tanks). The only component provided by BEG is the hydrogen low-pressure regulator.

Focus of the BEG system design has been the air system, cooling and E/E architecture up to the defined vehicle interfaces.

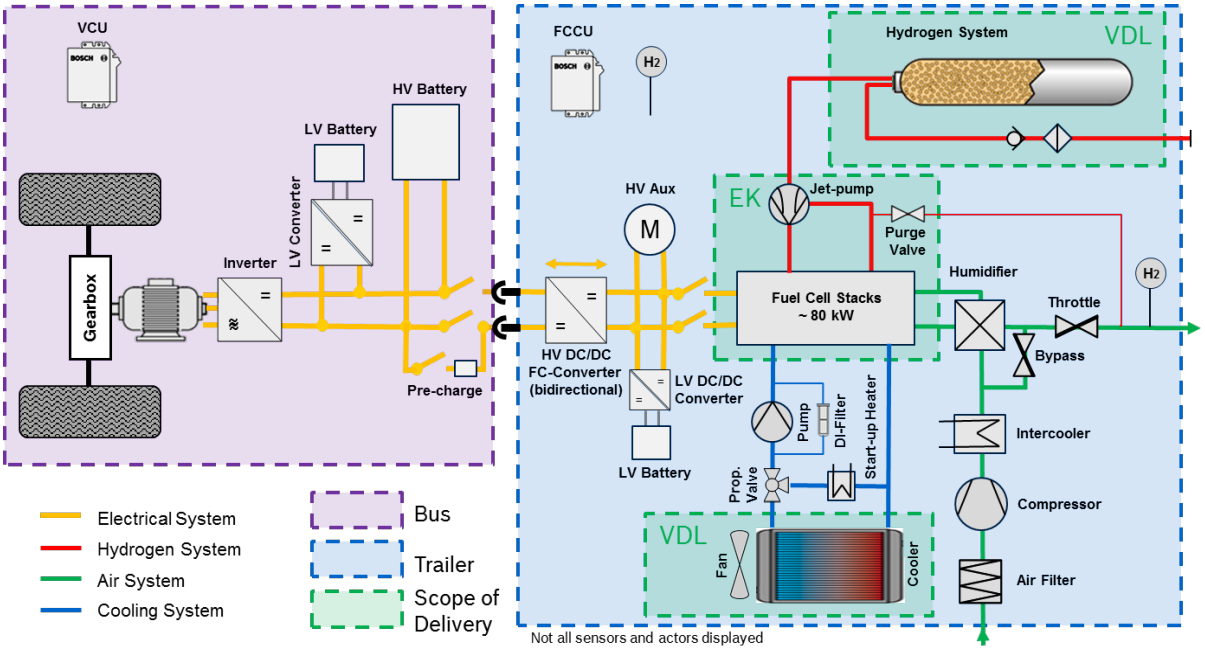

Fig. 2: System overview (2)

1.3 Scope

For any automotive product, endurance and low prices come with high production numbers. Since the expected volume of REEV electric busses will be comparatively low for the years to come, one of the focus aspects was for the BoP components to be readily available wherever possible.

Most of the components used are production parts, which are qualified for minimum passenger car requirements. Since fuel cell requirements differ from internal combustion engines, the choice for many components is quite limited in the current market situation. Hence, some solutions were chosen simply because they were the only one available.

In terms of performance over lifetime, ElringKlinger ran experiments considering stack degradation. The results will be considered in the development of the operational strategy. To get similar results for the BoP, three major components were chosen for closer consideration:

- Hydrogen low-pressure regulator Bosch HGI
- Intake air compressor Rotrex EC15-20
- Intake air humidifier Fumatech Ecomat H50

2 Description of Components

2.1 Hydrogen low-pressure regulator and metering valve Bosch HGI

In order to ensure proper functionality, high efficiency, and long lifetime of the fuel cell membrane, hydrogen pressure on the anode needs to be kept in a certain range in relation to both, ambient and cathode air pressure. In addition, the amount of hydrogen used needs to be fed into the anode system as accurately as possible.

In order to perform that task, Bosch developed an electronically controlled hydrogen injector valve HGI (Hydrogen Gas Injector). In combination with an anode pressure sensor signal, the Fuel Cell Control Unit (FCCU) controls the anode pressure and hence the amount of hydrogen used by means of this PWM operated solenoid valve.

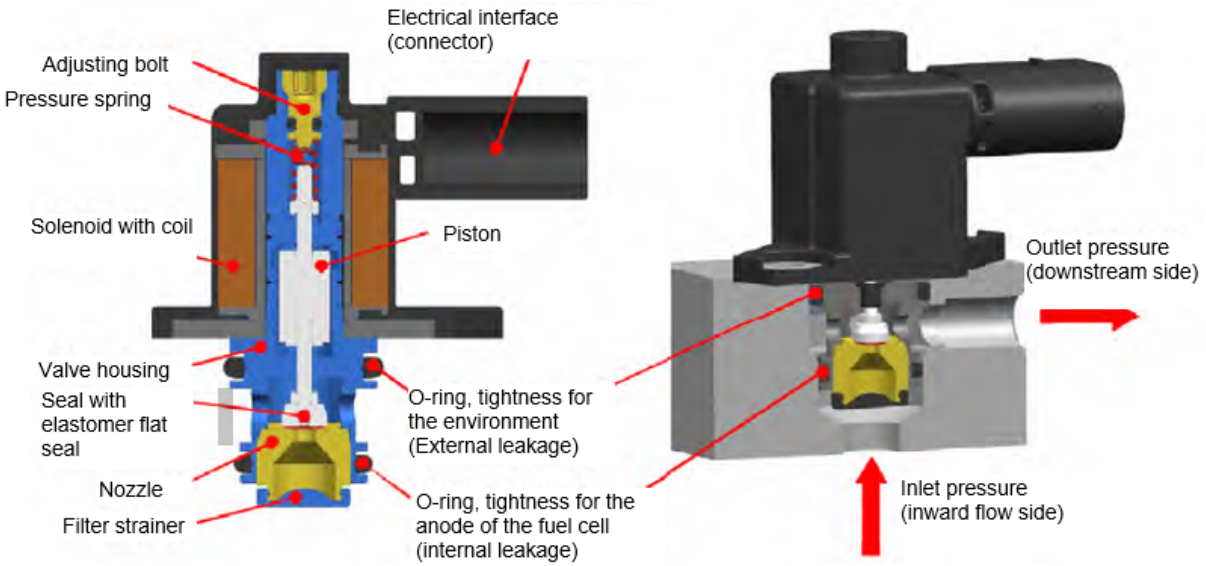

Fig. 3: Hydrogen injector valve (3)

2.2 Intake air compressor Rotrex EC15-20

For intake air supply, the system uses a Rotrex EC15-20 electric supercharger. This compressor is a standard automotive performance part and is usually driven by a poly-V belt. For use in automotive fuel cell systems, Rotrex remove the pulley and connect a Bosch SMG138 electric motor directly to the input shaft.

By means of a 1:12.67 “Traction Drive” transmission the impeller reaches a maximum of 180,000 rpm at 14,200 rpm motor speed and is capable of 150 g/s air mass flow and a maximum pressure ratio of 2.94 (4).

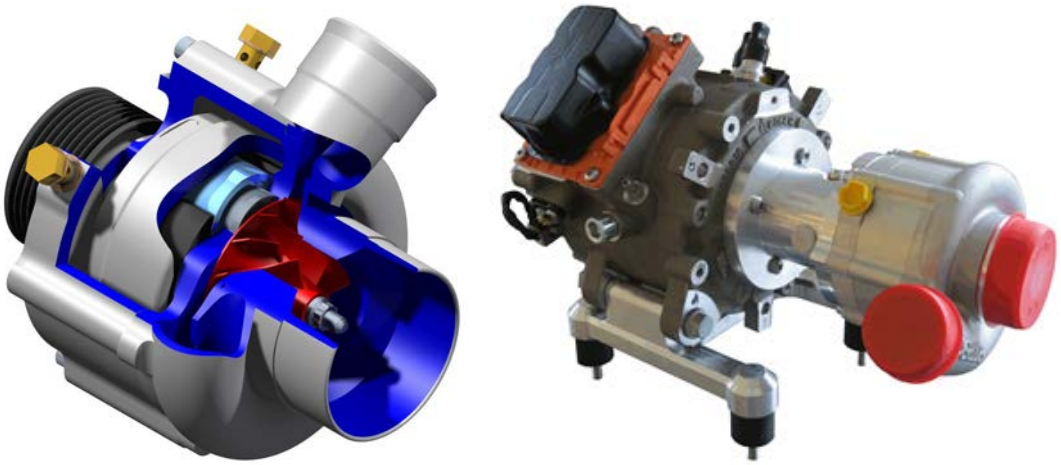

Fig. 4: Rotrex electric supercharger (5)

For lubrication and cooling, Rotrex supplies an additional oil circuit consisting of equalizing reservoir, oil filter, and heat exchanger. The oil pump is included in the compressor head unit. To ensure failure free operation, Rotrex specifies the use of Rotrex SX150 traction fluid by SantoLubes LLC. Since organic substances can encourage degradation of fuel cell membranes, the oil pump produces a slight vacuum so that air flows into the oil circuit rather than risk oil contamination of the compressed air. Nevertheless, in case of failure, oil spill cannot be ruled out completely.

2.3 Intake air humidifier Fumatech Ecomat H50

Before entering the fuel cell stack, the intake air needs to be humidified to prevent the membranes from drying. Giantleap system design uses a hollow fiber humidifier Fumatech Ecomat H50. Dry intake air flows through a main body containing 18 bundles of hollow membrane fibers and gets humidified by wet air from the fuel cell exhaust, that is being led around those fiber bundles.

Fig. 5: Fumatech Ecomate H50 humidifier

3 Analysis of components and ageing mechanisms

3.1 Hydrogen path component (HGI)

Endurance testing of the HGI has been done during the HGI development and showed no relevant degradation over lifetime. The development of the HGI was founded by the German National Organization for Hydrogen and Fuel Cell Technology NOW.

More information about that project can be found on the NOW homepage, project ID 03BI101. https://www.now-gmbh.de/en/

The final report (3), in German language, is linked there, too.

During this project, BEG did no further analysis and testing concerning the ageing and lifetime behavior of the HGI.

3.2 Air path components

As part of this work package BEG did detailed research and analysis concerning the ageing mechanisms of the main air path components air compressor and humidifier. Specialists dismantled both components, evaluated, and weighed the possible ageing mechanisms known from literature in order to define a test procedure carried out afterwards.

3.2.1 Air compressor

The Rotrex EC15-20 consists of the main functional components

- Bosch SMG 138 electric motor
- Oil system including rotary vane oil pump, oil cooler, filter an equalizing tank
- “Traction Drive” planetary gear
- Compressor volute and impeller

The Bosch SMG 138 is a permanently excited synchronous machine operated by a Bosch InvCon2.3 inverter. Since the motor speed and hence the compressor input speed is monitored and controlled by an integrated control module, a significant performance loss concerning the air supply system is not to be expected. Wear of bearings or residua caused by dirt can cause higher friction an increased power demand, leading to reduction in the systems net power.

Fig. 6: Bosch SMG 138 and InvCon 2.3

Both motor and inverter are automotive production parts and as such approved and field-tested for use in automotive applications. Any mechanical or electrical failure causing an increased power demand are monitored by the controller's diagnostic system.

As the electric motor, the performance of the oil system will not directly influence the air supply. Nevertheless, degradation of oil quality, contamination, or cooling issues can lessen the performance of the traction drive and bearings, causing increased power demand for the air supply system.

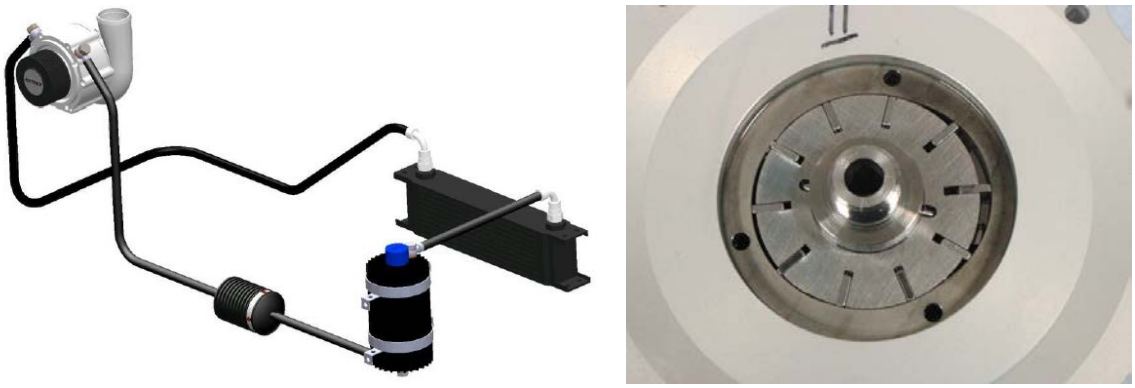

Fig. 7: Rotrex oil circuit ((5), left) and rotaty vane oil pump (right)

The air path components downstream of the compressor, especially the fuel cell membrane and catalyst, are sensitive to oil contamination. Since, after one component was damaged during transport, oil was found within the volute, the emission of traction fluid onto the process air needs to be considered.

The traction drive planetary gear is a patented Rotrex development and specified for the use with Rotrex SX150 traction fluid. Since there are no interlocking toothed wheels but shear and friction forces, the performance of the transmission depends directly on the properties of the traction oil, such as viscosity, temperature, chemical, or mechanical contamination. In addition to the condition of the traction oil, wear and tear inflicted on contacting surfaces and bearings will influence power and efficiency.

Fig. 8: "Traction Drive" transmission components - housing, planetary gear, cage

One main factor for the performance of the air supply system obviously is the compressor hear unit itself. Any change in the impeller or housing geometries over lifetime will influence the performance of the unit. Other than catastrophic failure of components, mainly erosion or buildup of soot on the impeller blades have to be considered.

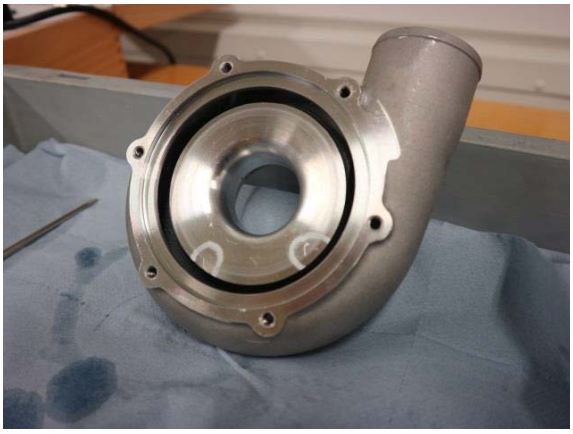


Fig. 9: Compressor volute (left) and impeller (right)

In order to protect the compressor from damage and prevent oil spill onto the air system, Rotrex specify the following (6):

- Intake air has to be filtered, so no particles above 20µm can enter the air system.
- The air filter must not block or be affected by mud or water at any time.
- Mounting angles and positioning of the compressor in relation to the oil path components are strictly limited.
- The oil used needs to fulfil Rotrex specification and has to be replaced after two years.
- The oil circuit has to be replaced completely after a major failure of the compressor.

General knowledge as well as literature research show various mechanical, chemical, and thermal factors that influence the performance of the compressor over lifetime, promote ageing or even cause premature failure of components.

Table 1: Classification of ageing mechanisms relevant for the compressor

Ageing mechanism	Cause	Classification
Fouling	Particles	Mechanical
Erosion	Particles, droplets	Mechanical
Fatigue	Vibration / shock, rotating stall, temperature, temperature differences	Mechanical, thermal
Wear and tear	Particles, droplets, insufficient lubrication	Mechanical
Corrosion	Gaseous or liquid contamination, soiling	Chemical

In addition to the factors mentioned above, also secondary effects need to be considered, such as insufficient lubrication or cooling caused by leakages or blockages. For a detailed description and evaluation, please consult chapter 4 of this report.

3.2.2 Humidifier

The Fumatech Ecomat H50 humidifier used for the Giantleap system is specified for fuel cell systems providing 50 kW up to 70 kW net power. Specifications allow for co- as well as counter-flow, while fresh air for the fuel cell supply always has to enter though the outer ports and will be led through the fibers and the wet exhaust has to run through the inner ports and around the fibers.

While the inner shell containing the fibers is fixed with both ports on the same side, both outside lids can be rotated by 180° so that one or both of the ports can be mounted to face in the opposite direction to give some flexibility in terms of package and routing of the pipes.

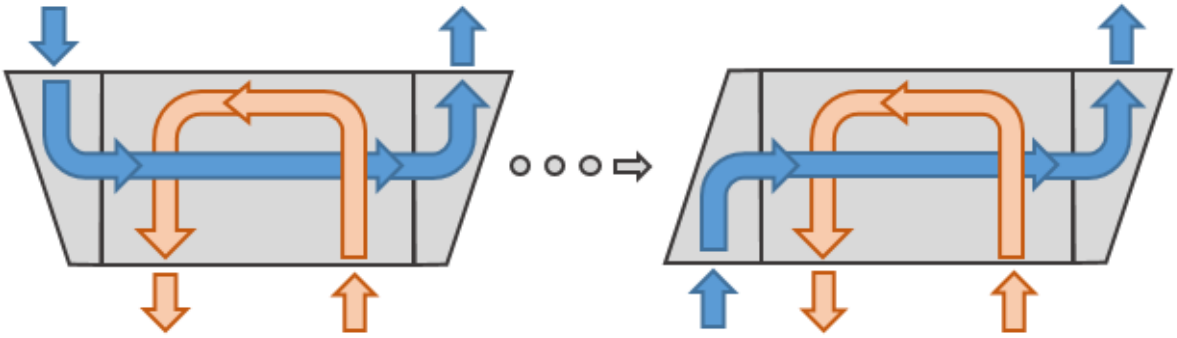

Fig. 10: Flexibility in mounting the humidifier endcaps

The inner shell consists of 18 bundles of hollow fibers mounted in some sort of resin inside a polyamide housing. The fibers have a medium wall thickness of 95µm. Both caps are made from polyamide and, as the shell housing, contain glass fibers for reinforcement.

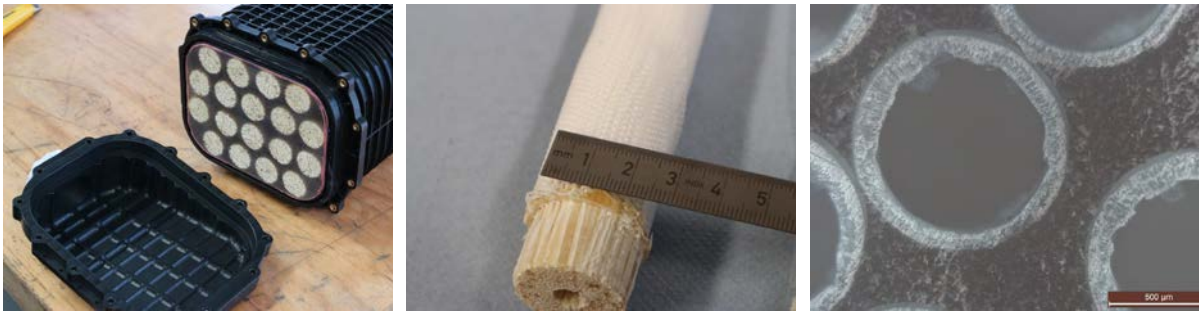

Fig. 11: Humidifier hollow fibers

To gain further information on the fibers' material, we ran some samples through a thermo-gravimetric analysis (TGA) as well as a differential scanning calorimetry (DSC).

For the TGA we heated a sample of about 6g from 20°C to 950°C and analysed the weight loss in relation to the temperature. For that process, a NETZSCH TG 209 F1 Iris thermal scale was used. The analysis shows some drying and evaporation of volatile substances with a weight loss of about 0.5% at 100°C and proves the material to be thermally stable till up to about 300…350°C. About half of the weight loss (47.8%) occurs rapidly between about 500°C and 600°C, the other half (49.1%) then deteriorates when heating up further. At 950°C, the leftover ashes contain 2.5% of the original weight.

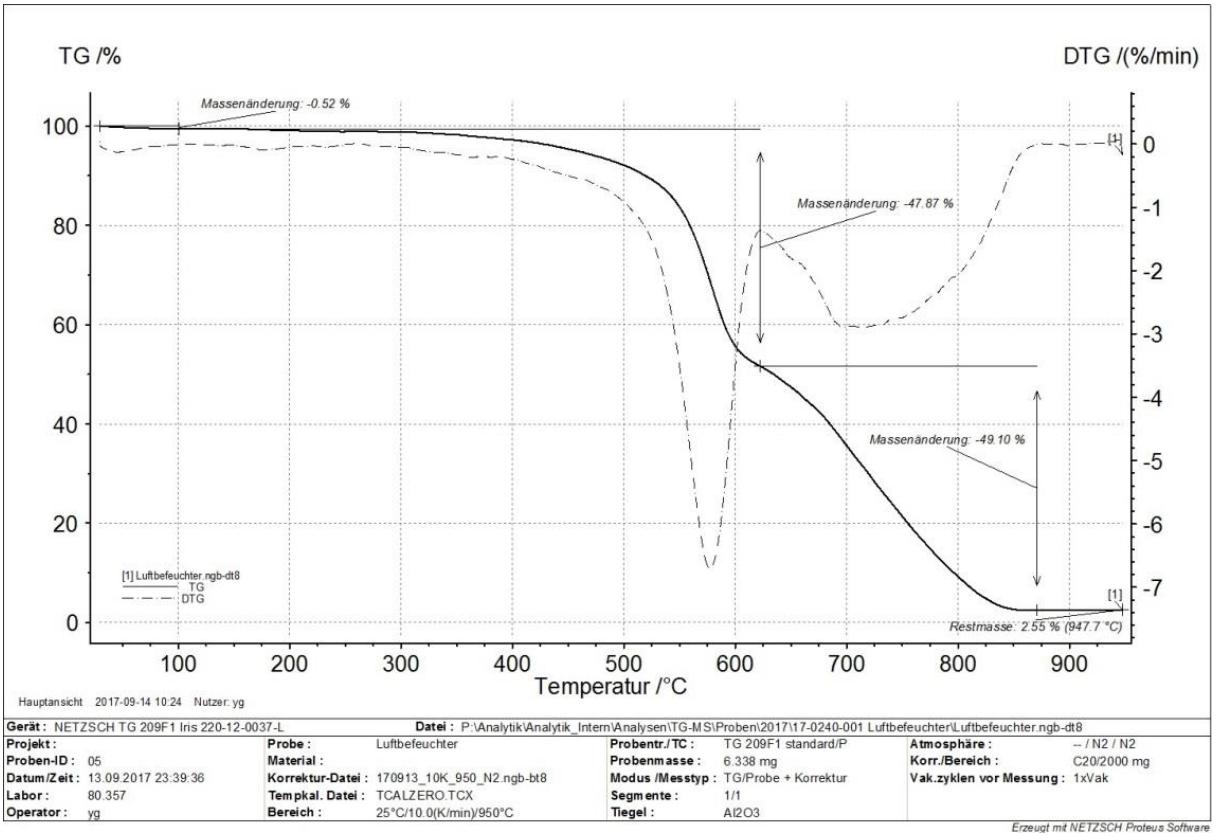

Fig. 12: Result of the thermo-gravimetric analysis

DSC evaluates the difference in heat flow between a material sample and an empty reference probe. As a result, changes in the physical properties of the examined material show in relation to temperature. In case of the humidifier's fibers, the glass transition temperature gives insight into the material used.

To determine the glass transition temperature, we heated the fibers' material from room temperature 25°C to 400°C at a rate of 10K/min and later cooled them back to 25°C at the same rate. Because of the bulky form, only very light samples could be used, so we repeated the process twice with samples of 1.952g and 2.566g respectively. Both measurements show glass transition at about 225°C. Fig. 13 shows the results is graphical form.

Both TGA and DSC do not give enough information to determine the material used exactly but show that it must be either polyether sulfone or polyether imide. Both materials are frequently used to produce membranes for various purposes.

Over lifetime, a decreasing efficiency of the humidification is expected. One major reason can be flooding of parts of the housing by liquid water. Since this is mainly influenced by design and mounting situation as well as operation strategy of the fuel cell system in total, this effect will not be examined here. Another reason for decreased performance can be blockage of fibers by frozen liquid water. Even though the humidifier will be frozen during the experiments conducted, we were not able to induce enough humidity into the test system to fully evaluate this effect.

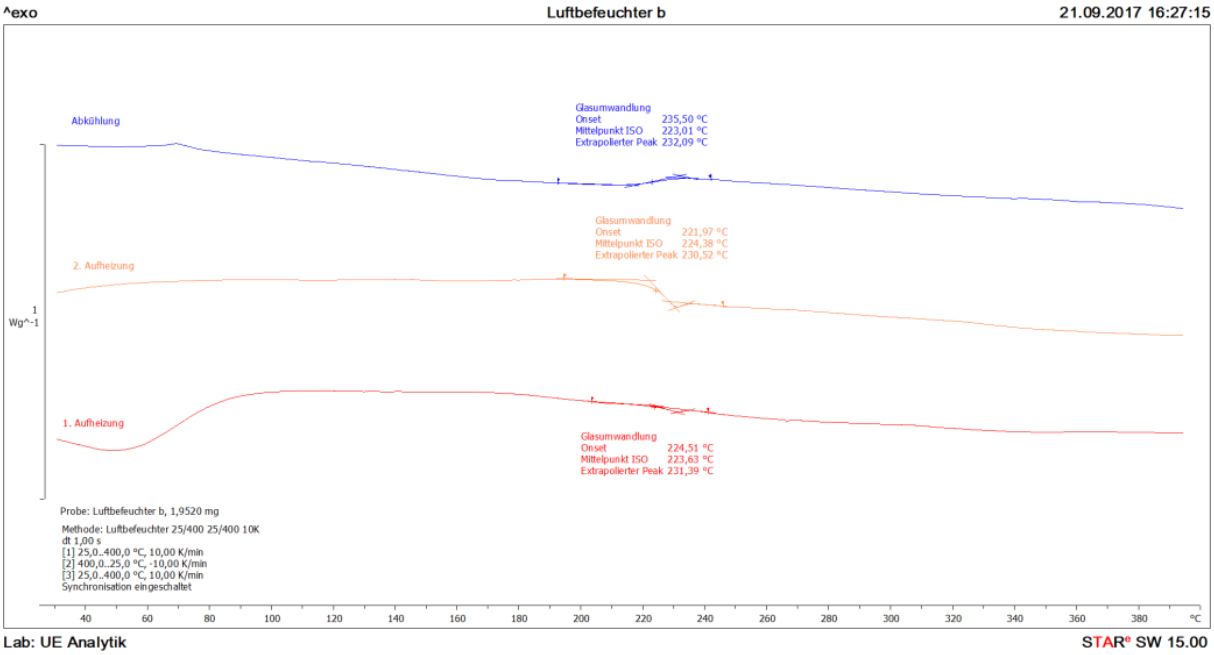

Fig. 13: Result of the differential scanning calorimetry

More relevant for this examination are performance losses caused by soiling of the membranes' surface, changes in material properties, or fatigue induced by mechanical influences, pressure differences, or thermal stress. Table 2 shows the main effects and mechanisms relevant for the ageing of the humidifier.

Table 2: Classification of ageing mechanisms relevant for the humidifier

Ageing mechanism	Cause	Classification
Fouling	Particles	Mechanical
Fatigue	Vibration / shock, temperature, temperature differences, pressure differences	Mechanical, thermal
Corrosion	Gaseous contamination, soiling	Chemical
Bio-contamination	Bacteria and micro-organisms	Mechanical, chemical

Bio-contamination might happen when bacteria and microorganisms grow in the humid warmth of the membranes' surfaces, causing clogging of the pores and corrosion of the material itself and so reducing the humidification efficiency. Since this mechanism is difficult to simulate, it needs to be kept in mind for the evaluation of the field tests.

The experiments will follow the specification boundaries given by Fumatech:

- Maximum intake air temperature = 110°C
- Maximum intake air pressure = 3.0bar$_a$

There is no explicit demand for the intake air to be filtered, so for the humidifier the same specification will apply as for the compressor.

4 Evaluation of ageing mechanisms

4.1 Compressor

As mentioned above, various mechanisms have been identified that contribute to performance losses of the compressor over lifetime. Fig. 14 shows a summary. During the following paragraphs, those will be described and evaluated in order to define experiments to facilitate accelerated ageing of the component.

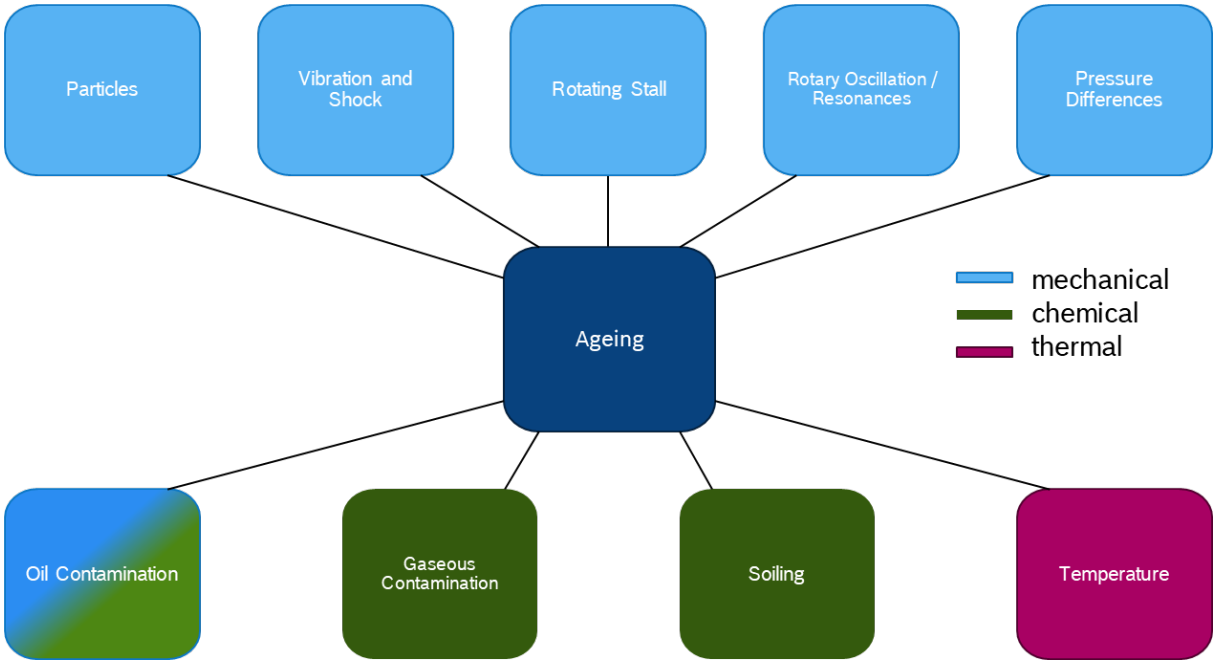

Fig. 14: Factors responsible for ageing of the compressor

4.1.1 Particles

Particles get transported into the air path with the intake air and will affect the mechanical integrity of the components. Particles with a diameter smaller than 10 µm might lead to fouling, agglomeration of those particles on the rotor blade surfaces. This will cause deterioration of the aerodynamic properties of the air compressor, imbalance of the rotor and thus higher structural load towards materials and bearings.

Larger sized particles will cause erosion and wear on surfaces exposed to the airflow. In addition to the consequences mentioned above concerning aerodynamic and mechanical properties, this might also cause increased contamination of other components further down the air path, including the fuel cell stack itself (7) (8) (9) (10).

Due to specifications, no particles larger than 20 µm in diameter can pass the filter. For Giantleap, the fuel cell system is intended to be used on public inner-city roads, so significant air pollution is to be expected, but no dust load that may affect the performance of the filter.

4.1.2 Vibration and shock

Since the Components will be mounted in a vehicle operated on public roads, they will be exposed to vibration and shock caused by outside stimuli as well as by sources within the system itself. This will

enhance wear of bearings and fatigue in structural components, leading to performance loss up to mechanical destruction of the component (11) (12) (13) (14) (15).

Both the Rotrex compressor unit and the Bosch electric motor have been designed and tested for automotive use. BEG experts also do not expect a continuous loss of performance due to vibration or shock rather than spontaneous failure of the component, so we decided on not spending the effort of testing the Rotrex compressor on a shaker unit.

4.1.3 Rotating stall

For a turbine air compressor, rotating stall and pressure differences are in close relation. If the pressure ratio at a given air mass flow gets too high, air starts to surge back against the rotation, destroying the impeller in the process. While the compressor map specifies the surge line and forbidden areas of operation, depending on the pressure needed, the compressor might be operated very close to that line. This can lead to rotating stall, pulsations within the air column, which will induce oscillation in the rotor blades. In addition to a loss of performance, material fatigue and increased wear of bearings can be caused (16) (17).

Since any PEM fuel cell stack needs a certain air pressure for efficient operation, the test procedure includes operation points that are close to the compressor surge line.

4.1.4 Rotary oscillation and resonances

Fluid kinetic compressors for automotive use run at a very high speed of more than 100,000 rpm. During manufacturing, a very precise balancing of the impeller shaft is crucial. Oscillations caused by rotor imbalance, resonances as worst case, will cause increased wear of bearings and fatigue in structural components (18).

The compressor also will operate above its resonance frequencies. Specifications demand a minimum idle speed of 3,000 rpm motor, equal to just less than 40,000 rpm impeller, that may not be undercut. In order to cover as much influences as possible, the test cycle includes operation at idle as well as high load.

4.1.5 Pressure differences

In addition to surging and rotating stall, pressure differences can cause cavitation. This effect can cause massive erosion in components pumping liquids. For gaseous media cavitation does not occur, so this effect can be neglected for the compressor.

4.1.6 Oil contamination

Since the Rotrex compressor contains roller bearings that are lubricated by oil, oil contamination needs to be considered. Mechanically, oil contamination can increase wear in bearings. Additionally, particles could cause clogging of the oil cooler (19) (20).

In addition to mechanical wear, oil contamination with aggressive chemical substances could enhance corrosion within bearings, transmission oil pump etc. Therefore, performance will drop due to higher friction losses. If seals are affected, traction oil might be spilled into the air path, affecting other components.

4.1.7 Gaseous contamination

Aggressive chemical substances might cause corrosion or decrease of material properties in components that are in contact with the intake air.

The fuel cell itself demands for the intake air to be filtered chemically and be void of aggressive substances. Hence, for the compressor, the influence of aggressive gaseous substances is considered negligible.

4.1.8 Soiling

In addition to mechanical effects, soiling of components like rotor blades might induce corrosion. As, for the materials used in a fuel cell system, the demand for chemical resistance is very high, corrosion caused by soiling is not considered as a major factor for degradation. Rotrex specification though asks for regular maintenance of the oil circuit in order to prevent damages in transmission or bearings due to impurities (21) (22).

4.1.9 Temperature

In terms of thermal effects, very high and very low temperatures need to be considered. For the mechanical integrity of the compressor itself, we expect fatigue caused by thermal stress and loss of material properties due to extreme temperature conditions to cause spontaneous failure rather than permanent degradation.

For the oil circuit, temperature will possibly affect the lubrication property. While low temperature will cause high viscosity of the compressor's traction oil and thus insufficient lubrication, high temperature might generate chemical and physical degradation of the oil itself. Both, over lifetime, will influence wear and tear of transmission and bearings (20) (23).

Fig. 15 shows the viscosity of the Rotrex SX150 traction fluid in correlation to temperature.

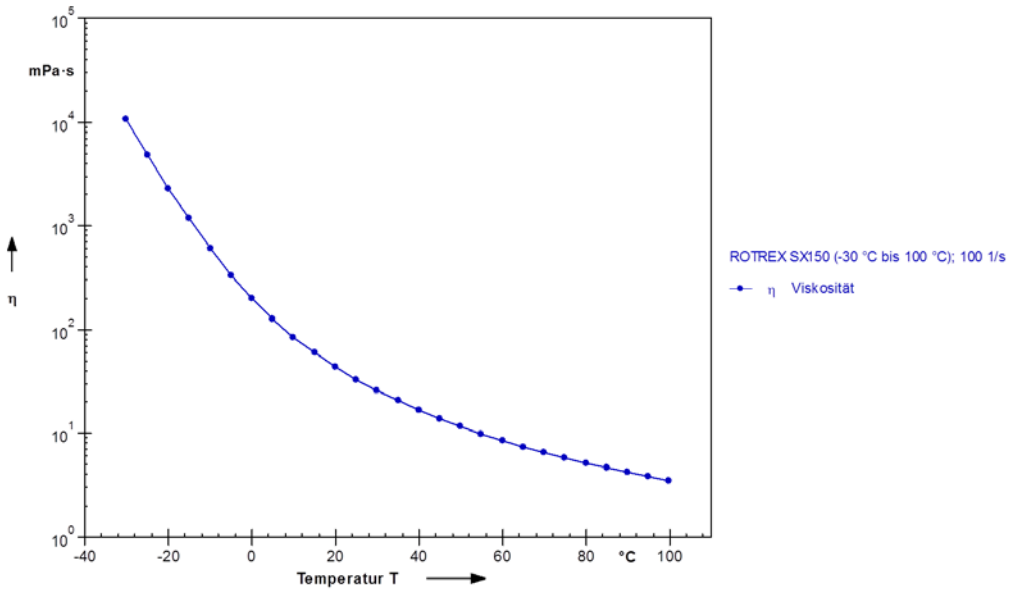

Fig. 15: Viscosity of the Rotrex SX150 traction fluid

The test cycle considers hot conditions as well as freezing.

4.1.10 Evaluation table compressor

Table 3 gives an overview of the relevant factors for the degradation of the air compressor during lifetime.

Table 3: Evaluation of ageing mechanisms – overview compressor

Relevant Factors		Mechanism Responsible for Ageing			Evaluation		
		mechanical	chemical	thermal	Literature	Operation	Evaluation
Particles (2-10µm)	→	Fouling			(7) (8)	Air Filter: < 20µm	o
Particles (>10µm)	→	Erosion			(9) (10)	Air Filter: < 20µm	-
Vibration / Shock	→	Fatigue			(11) (12) (13)	DIN ISO 16750 DIN EN 62506	+
Vibration / Shock	→	Leakage			(14) (15)	DIN ISO 16750 DIN EN 62506	+
Rotating Stall	→	Fatigue			(16) (17)	Operation close to Surge Line	+
Rotary Oscillations	→	Fatigue			(18)	o	o
Pressure differences	→	Cavitation			-	-	-
Gaseous Contamination	→	Cavitation	Corrosion		-	CO2 < 1% CO < 35ppm NO_x < 10ppb SO_x < 1ppb	-
Soiling	→	Abrasion	Corrosion		(21) (22)	Humidity	+
Oil Contamination	→	Clogging Wear	Corrosion	Increased Temperature Level	(19) (20)	Closed Oil Circuit, Oil Filter	-
Leakage	→	Abrasion		Increased Temperature Level	(24)	Closed Oil Circuit, Oil Filter	-

Temperature	→		Oil Degeneration	Fatigue, Abrasion, Particle Fusion	(20) (23)	Oil Temperature < 80°C	-
Temperature (< 0°C)	→	Wear			(20)	Rotrex Traction Fluid > -40°C	o

4.2 Humidifier

As for the compressor, also for the humidifier the ageing mechanisms have been identified as shown in Fig. 16 and will be subject to further evaluation in the following paragraphs.

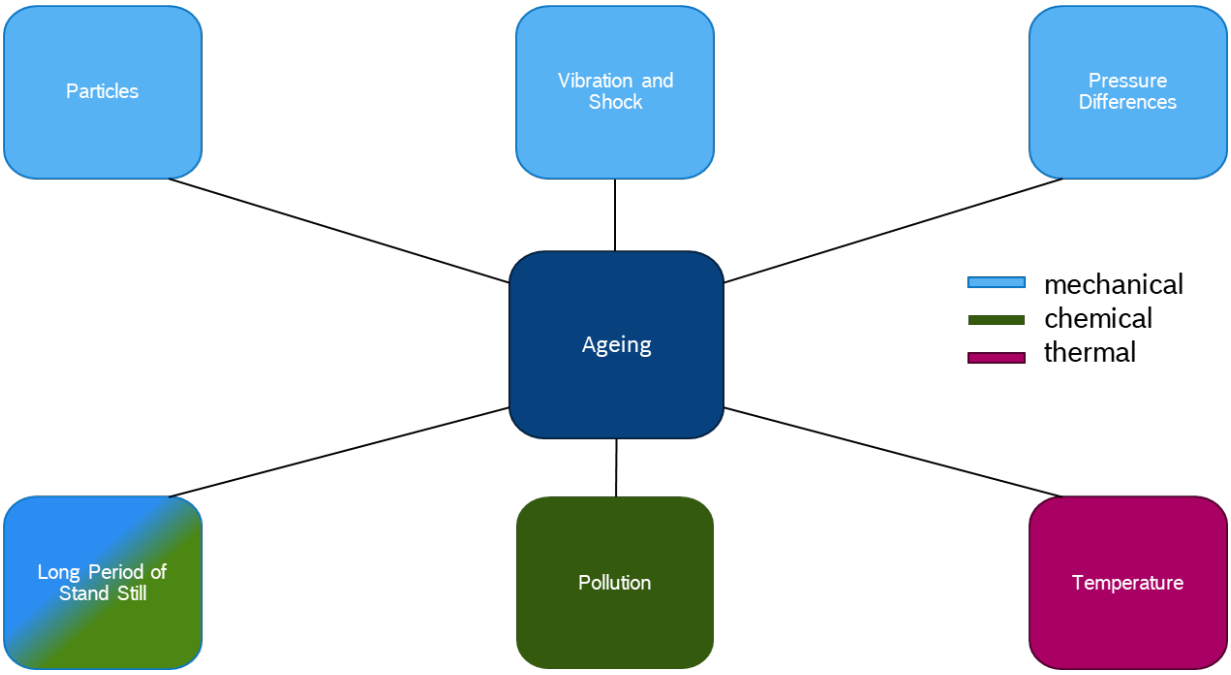

Fig. 16: Factors responsible for ageing of the humidifier

4.2.1 Particles

Within the humidifier, particles of any size will encourage clogging of the membranes' pores or even complete channels, so active surface and with it, performance will deteriorate.

The intake air will be filtered, so only particles of small diameters have to be considered. For now, no use of the fuel cell system in a dust heavy environment is planned.

4.2.2 Vibration and Shock

Vibrations put stress on outside mounting points of the housing as well as the internal structure of the humidifier. Next to spontaneous failure, also continuous performance losses due to cracks in single fibers, cracks in the resin separating intake and exhaust areas, or loosening of the mounting points of the fibers within the resin have to be considered.

Vibration testing has not been conducted in this project for various reasons but will be subject of further development.

4.2.3 Pressure differences

Pressure difference over the membranes and pressure gradients we consider the main reason for stress on the mechanical properties of the fibers leading to structural weakening of the material. Next to soiling of the surfaces this might be one of the main reasons for performance losses of the humidifier.

The test cycle will contain operating points with high as well as low pressure, according to the operation strategy intended for the vehicle.

4.2.4 Long periods of standstill

Fuel cell systems create a warm and wet environment. Depending on the level of contamination, nutrients deposited on the surfaces might encourage growth of bacteria and microorganisms. This will diminish the active surface and, depending on the contamination, might even influence the mechanical and chemical properties of the membrane itself. In this case, long periods of standstill will also influence the performance of membranes.

The effect of bio-contamination on membranes cannot be examined in this project but needs to be considered in further studies, especially since it will influence the fuel cell MEA as well.

4.2.5 Pollution

In addition to blocking active surface, pollution of the component can enhance chemical degradation of the materials, too. Under the requirement that the air be chemically filtered, this effect can be neglected for the humidifier.

4.2.6 Temperature

Low temperature can cause freezing of trapped humidity and so crack the structure of the membranes. Temperatures too high will damage the structural integrity of the material itself, changing the properties in terms of diffusion or even burning or melting the fibers (25) (26) (27) (28).

In the Giantleap system, all components will run within their specifications. During the testing procedure, a temperature range between -30 and 110°C will be covered.

4.2.7 Evaluation table humidifier

To give an overview, the factors mentioned above are summarized in Table 4.

Table 4: Evaluation of ageing mechanisms – overview humidifier

Relevant Factors		Mechanism for Ageing			Evaluation		
		mechanical	chemical	thermal	Literature	Operation	Evaluation
Particles (2-10µm)	→	Fouling			-	+	-
Particles (>10µm)	→	Erosion			-	-	-
Vibration / Shock	→	Fatigue			o	o	o
Pressure differences	→	Fatigue			o	DSC (<223°C)	o
Extended Stand-Still	→	Fouling			-	-	-
Pollution	→		Corrosion		o	CO2 < 1% CO < 35ppm NO_x < 10ppb SO_x < 1ppb	-
Temperature	→		Change of Material Properties		(26) (27) (28)	~ 100°C	-
Temperature	→			Fatigue	(25)	~ 100°C	+

5 Definition of test cycle and test bench set up

5.1 Standard for accelerated ageing

To accelerate the ageing of a component or system, said component or system is run under operating conditions that contribute to performance losses over lifetime, with all conditions left out that do not cause any harm. German and European standard DIN EN 62506 (29) describes methods for accelerated testing. In different stages of the product development cycle, different types of tests are defined to help verification of product durability.

The standard defines three types of test to be executed in parallel in order to assure production maturity (29):

- Type A: Qualitative accelerated tests for detection of failure mode and/or phenomenon
- Type B: Quantitative accelerated tests for prediction of failure distribution in normal use
- Type C: Quantitative time and event compression tests for prediction of failure distribution in normal use

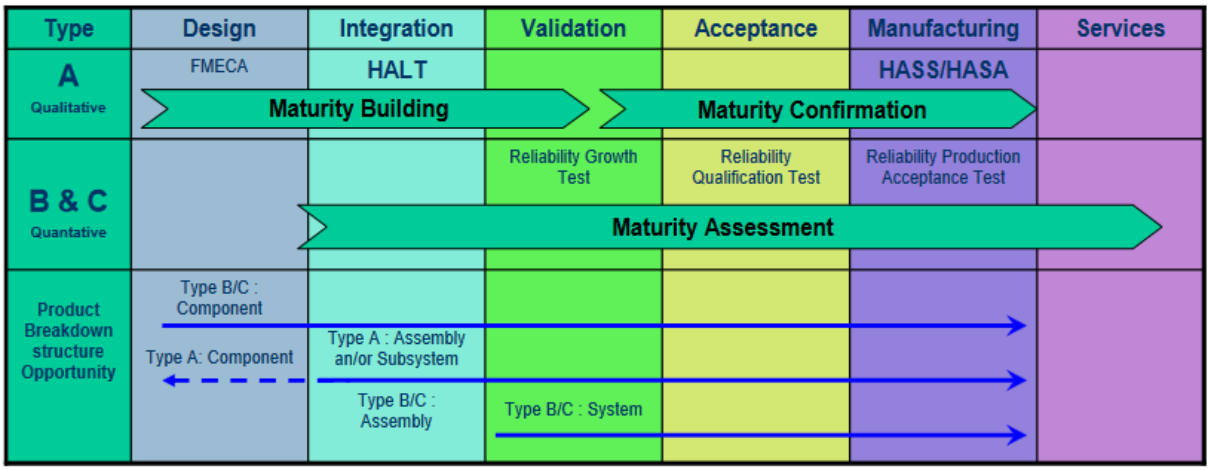

Fig. 17: Test types mapped to the development cycle of a product (29)

While type A uses test with strongly elevated load in order to show systematic weaknesses in design, types B and C require a rather high number of test specimen, so statistic distribution of failure can be shown. Since only one piece of each component was available for the test, we did not define the test procedure according to DIN EN 62506 strictly, but still used it as a guideline to help fixing the test parameters.

During all testing, we took care not to run any component outside its specified operation range in order to not damage parts due to overstrain.

5.2 Evaluation of in-use conditions

Manufacturers of commercial vehicles typically ask for a lifetime of 30,000 hours for the systems used in their vehicles. For Giantleap however, the period planned for demonstration is considerably shorter.

In order to estimate the power required from the fuel cell system, VDL provided a chart with the simulated load profile of an inner city 12-meter bus as shown in Fig. 18. Next to other calculations, we also used this data to adapt a load cycle for the BoP test bench.

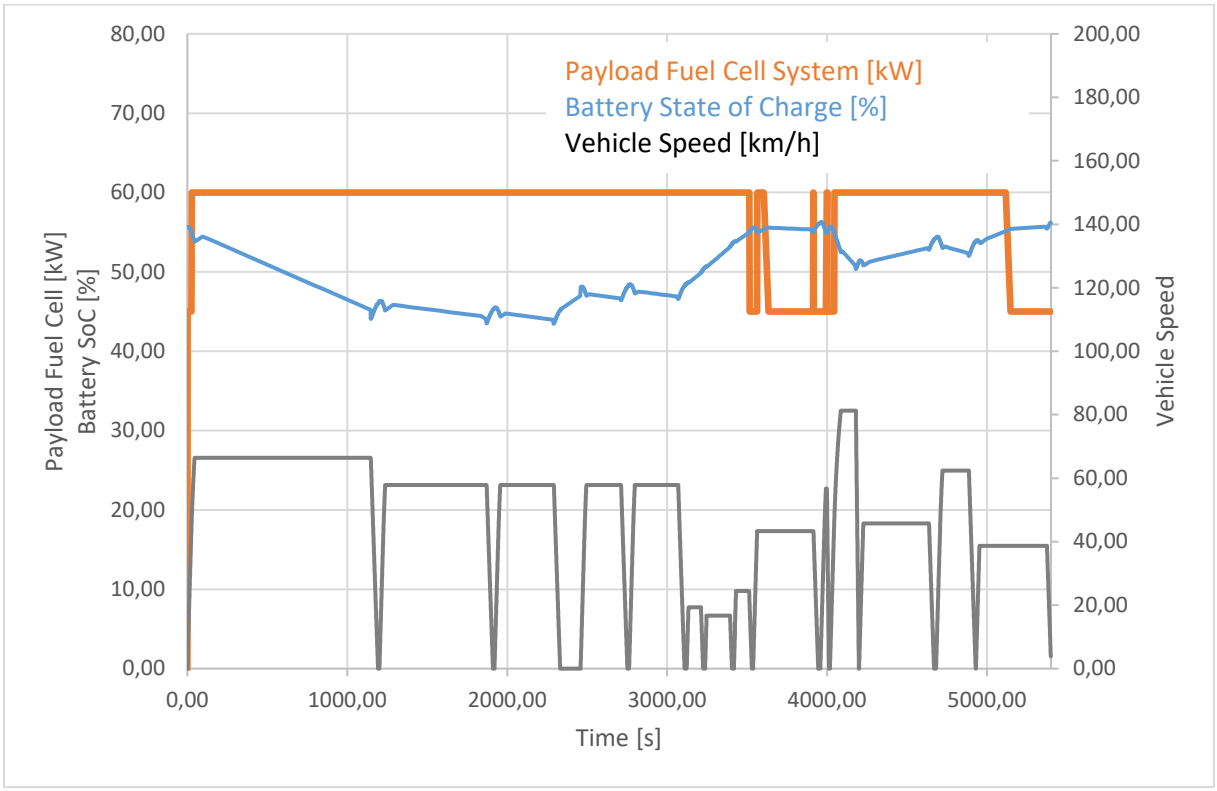

Fig. 18: Simulated power output of the fuel cell system for the demonstration vehicle

Based on the data provided, we assumed from 5,400 s = 1.5 h a daily use of 5 cycles, amounting to 9 hours including short breaks in between each cycle. Given a use of 300 days per year and a 3 year period of demonstration for the prototype vehicle, this amounts to a total of 8,100 hours of use. For the test program, the cycle shown above was simplified and reduced to a basic daily cycle shown in Fig. 19, which then was the basis for the test bench set-up.

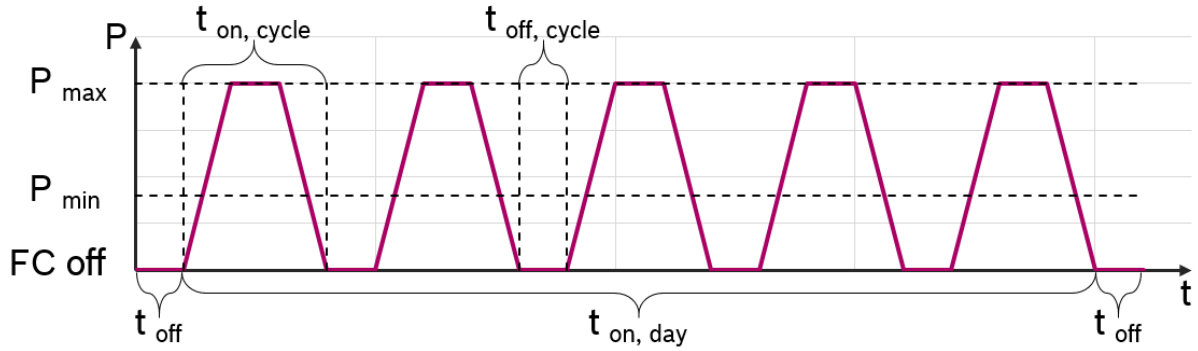

Fig. 19: Daily in-use cycle for test bench set-up

From those considerations, we estimated all the parameters used to define the test procedure as listed in Table 5.

Table 5: Parameters used to define test conditions

Parameter	Symbol	Value	Source
Total duration of use	t_0	8,100 h	Estimation, based on VDL Input
Reliability demand	$R_0(t_0)$	0.85	
Total time running	t_{on}	5,000 h	Estimation, based on VDL Input
Total time standstill	t_{off}	3,100 h	Estimation, based on VDL Input
Time running per day	$t_{on,\ day}$	9 h/d	Estimation, based on VDL Input
Number of cycles per day	N_{day}	5	Estimation, based on VDL Input
Total number of cycles	N	4,500	
Maximum ambient temperature	T_{max}	40 °C	Definition, based on experience
Medium ambient temperature	T_{avg}	11 °C	VDI 4710-4
Minimum ambient temperature	T_{min}	-15 °C	Definition, based on experience
Air relative humidity maximum	$RH_{on,\ max}$	95 %	
Air relative humidity minimum	$RH_{on,\ min}$	20 %	

Minimum and maximum ambient temperatures are based on background knowledge in automotive product development combined with what is to be expected for the demonstration vehicle. Also we made use of data available in guideline VDI 4710-4 published by the German Association of Engineers, that gives weather data for 122 European cities in a time period of 15 years from 1991 to 2005. The following graphs Fig. 20 and Fig. 21 show as an example the temperature date for the locations (or close by), where Giantleap partners are situated.

While in this case Trondheim, Norway and Split, Croatia give the left and right boundaries for the northernmost and southernmost cities, the Central European locations show a 50 % value at 11 °C. This temperature was chosen as standard ambient temperature for the test bench set-up.

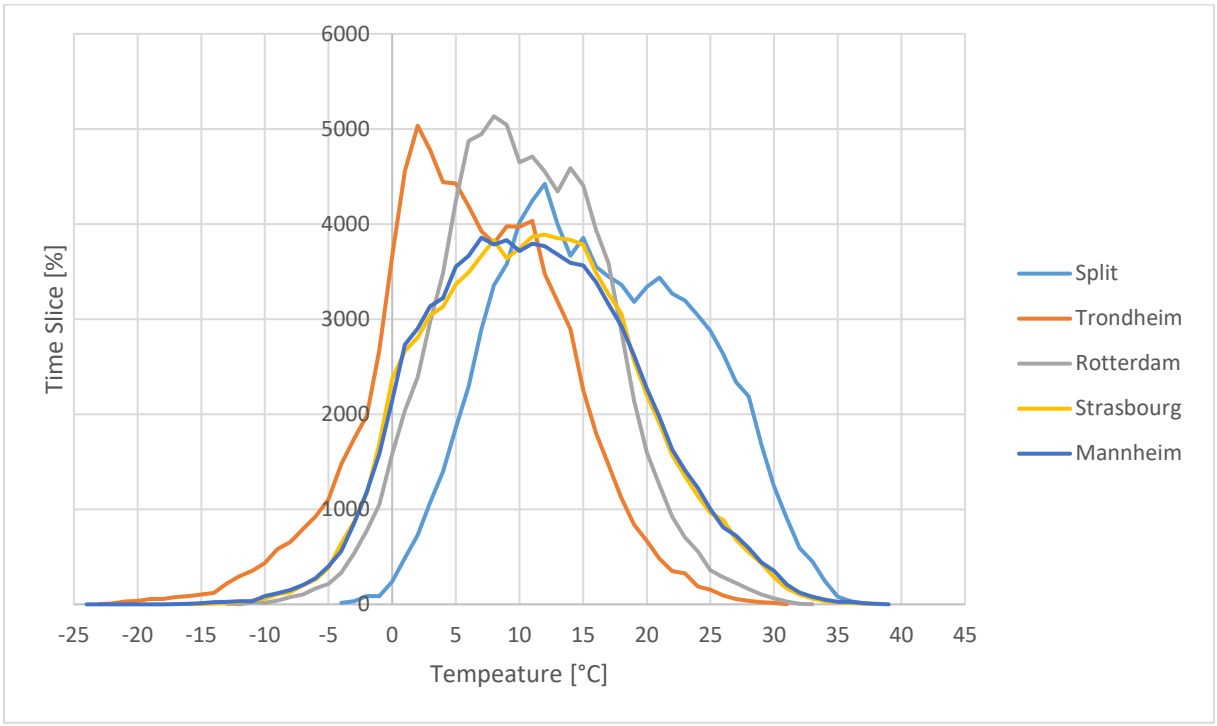

Fig. 20: Temperature distribution for locations of Giantleap partners

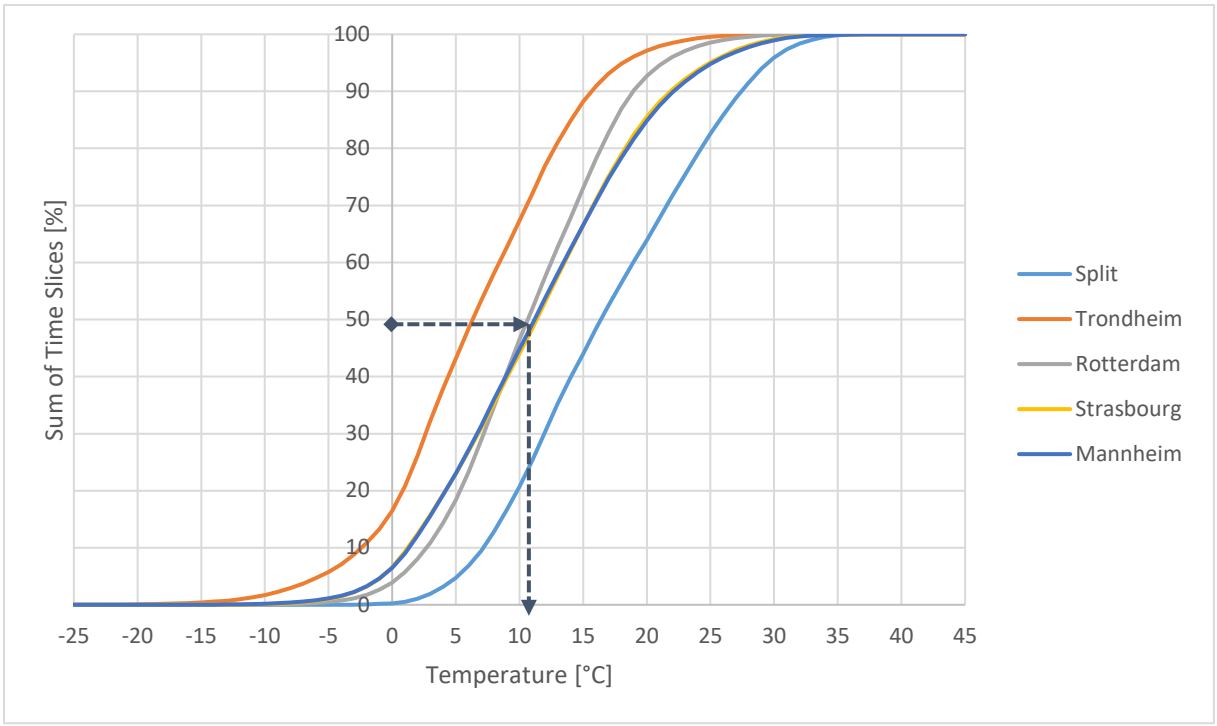

Fig. 21: Temperature distribution summarized

5.3 Test bench set-up

To facilitate the test, BEG hired a climate-controlled test chamber normally used for hot gas examination, located at Fraunhofer institute in Karlsruhe, Germany. To save time and cost, we decided to test the whole cathode path in one set-up, so the whole assembly of compressor, charge air cooler, humidifier war mounted onto a cart. In order to control all the parameters necessary, various conditioning units could manipulate temperature, humidity, and pressure.

Via temperature, pressure, and humidity sensors, the test bench controller was able to both monitor and manipulate the relevant parameters and store measurement data for further assessment and evaluation. Table 6 describes the relevant nomenclature for the set-up while Fig. 22 gives a graphical overview. A complete list of the sensors used can be found in Appendix A: List of measuring points.

Table 6: Nomenclature for test bench set-up

Label	Description	Parameters monitored	
ENV	Environmental conditions	Ambient pressure, temperature, and humidity	
COM	Compressor Rotrex EC15-20	Air temperature and pressure, both intake and outlet, Relative humidity, air mass flow, vibrations	
CON1	Charge air cooler	Air temperature	
HUM	Humidifier Fumatech Ecomate H50	Air temperature, pressure and humidity for all 4 ports, Air mass flow	
CON2	Conditioning unit 2	Air temperature, humidity	Fuel cell stack simulation
BPU1	Back pressure unit 1	Air pressure	
BPU2	Pressure control valve	Air pressure	
GEA	Compressor gears and oil pump	Oil temperature, pressure and mass flow	
CON3	Conditioning unit 3	Oil temperature, coolant temperature	
EM	Compressor electric motor	Voltage, current, power, speed	

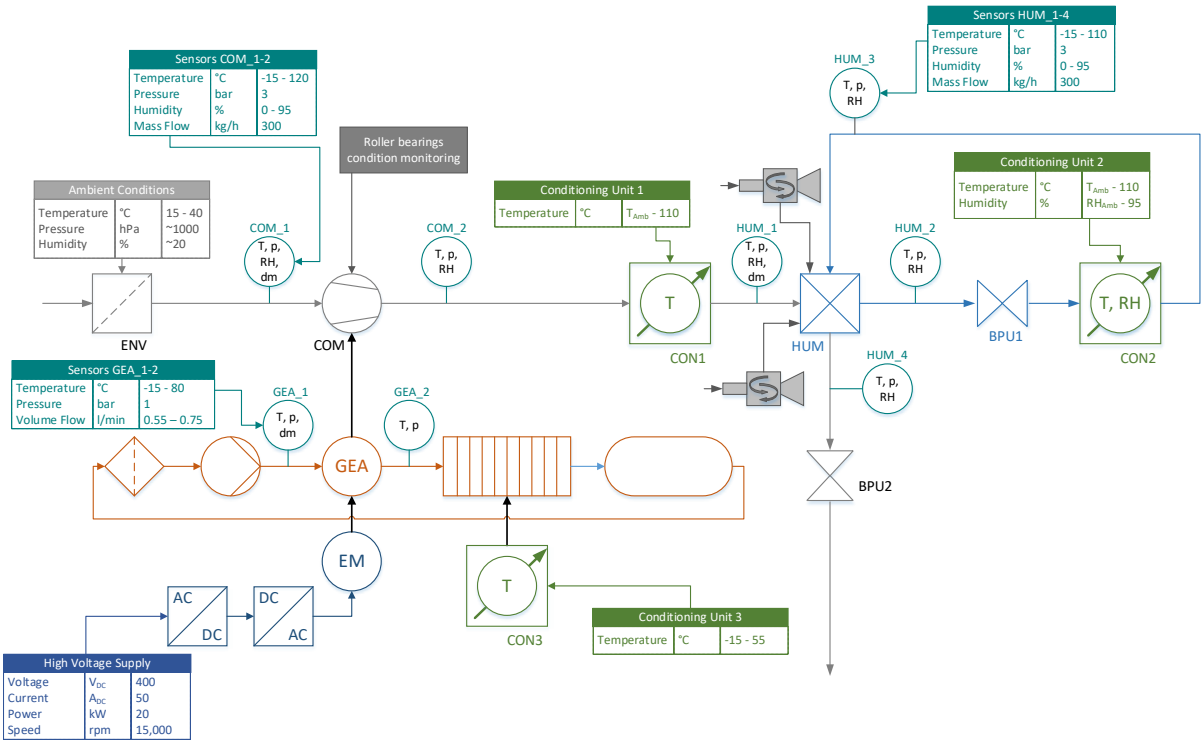

Fig. 22: Test bench schematics

While condition units CON1 and CON3 are heat exchangers with the temperature controlled by a water cooler, CON2 includes an electrical heater an a spray nozzle for liquid water. CON2 simulates the fuel cell stack and provides the humidity for the humidifier HUM to work with.

In order to provide additional cooling power, port one and three of the humidifier were connected to one vortex tube each. Driven by compressed air, those tubes could provide additional cooling for the cold phases down to -20°C. “The vortex tube, also known as the Ranque-Hilsch vortex tube, is a mechanical device that separates a compressed gas into hot and cold streams. […] It has no moving parts. (30)”

Fig. 23: Separation of cold and hot steam in a vortex tube (30)

Since the compressor runs on roller bearings, we mounted a triple-axis acceleration sensor on the housing to get information in the bearing condition. The test-bench measurement unit, next to storing the raw data from the sensors, also provides a characteristic value for the condition of the bearings by the evaluation of Spike Energy, a known principle for condition monitoring of roller bearings (31).

The temperature inside the humidifier was an important control quantity as well as a highly interesting measurement parameter giving insight into to conditions inside the fibers. Hence, thermo-couples were inserted into the ports as well as into the fiber bundles as shown in Fig. 24 and Fig. 25.

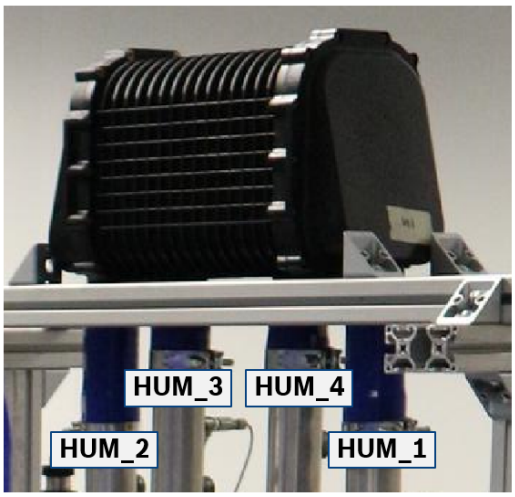

HUM_1: Dry air intake

- Active cooling by Vortex pipe during cold phase
- Compressed air conditioned by air cooler

HUM_2: Humidified air

- Air humidification by humidifier test sample

HUM_3: Wet air from FC

- Active cooling by Vortex pipe during cold phase
- Active heating during hot phase
- Evaporation of water

HUM_4: Exhaust

- Air de-humidified by humidifier test sample
- Pressure regulation by back pressure unit

Fig. 24: Measuring points HUM_1-4 in the humidifier ports

Fig. 25: Measuring points HUM_005, HUM_009, HUM_012, and HUM_015 in the humidifier fibers

5.4 Test cycle

The analysis of compressor and humidifier suggested two different test cycles, specialized on the specific ageing mechanisms of the two components. The following figures Fig. 26 and Fig. 27 describe those individual cycles.

Compressor

- Total Time of Testing: 450 h
- Total Number of Cycles: 160
- Cover Extrema by Cold and Hot Cycle

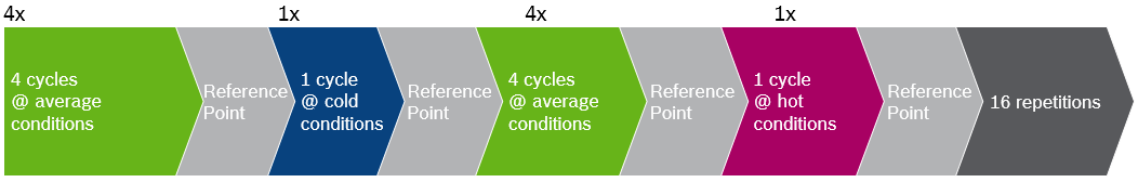

Parameter	Reference Point	Average Cond.	Cold Conditions	Hot Conditions
$T_{Oil\ min}$	20°C	11°C	-15°C	11°C
$T_{Oil\ max}$	20°C	55°C	55°C	80°C
Pressure ratio	1,5	2	2	2
Mass flow Air	140 g/h	280 g/h	280 g/h	280 g/h
Comment				Inject 1,1 g Water

Fig. 26: Specific test cycle for the compressor

Humidifier

- Total Time of Testing: 454 h
- Total Number of Cycles: 404
- Cover Extrema by Cold Cycle

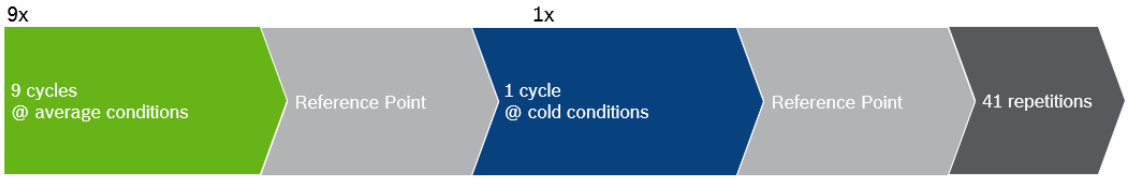

Parameter	Reference Point	Average Cond.	Cold Conditions
$T_{Housing\ min}$	65°C	11°C	-15°C
$T_{Housing\ max}$	65°C	110°C	110°C
Pressure	1,5 bara	2 bara	2 bara
Mass flow Air	233 g/h	280 g/h	280 g/h
Humidity	RH_{in} dependent on ambient conditions, RH_{out} = 95%		

Fig. 27: Specific test cycle for the humidifier

As mentioned above, in order to choose a more pragmatic approach, we decided to test both components in one single test, so a test cycle had to be defined, that covers the specific demand for both components. This cycle needs to cover

- Average conditions in terms of temperature and pressure
- Cold temperature conditions and freezing
- Hot temperature conditions
- High- and low-pressure conditions
- High temperature and pressure gradients / thermo-shock
- Operation close to the compressor's surge line
- Reference point for clearly defined reference measurement

Those considerations, together with lessons learned from the implementation, lead to the definition of the test cycle. The parameters are listed in Table 7.

Table 7: Parameters of test cycle

Phase		Temp. Humidifier	Air Pressure	Air Compressor Impeller Speed	Stop Criterion	
1.	Cold Phase	10°C	~ p_{Amb}	60,000 rpm	Event	All T_HUM < 15°C
2.	Hot Phase	100°C	2.5 bar_a	155,000 rpm	Time	40 minutes
3.	Reference Point	80°C	1.9 bar_a	135,000 rpm	Time	10 minutes
4.	Surge Line OP	80°C	2.05 bar_a	135,000 rpm	Time	1 minute
5.	Sub-Zero Phase	-15°C	~ p_{Amb}	60,000 rpm	Event	All T_HUM < -10°C
6.	Thermo-Shock Hot	100°C	2.05 bar_a	145,000 rpm	Time	5 minutes
7.	Thermo-Shock Cold	-15°C	~ p_{Amb}	60,000 rpm	Time	5 minutes

During cold and sub-zero phases, the compressor is still operated with low speed, on the one hand, because low speed also was defined as a possible ageing mechanism, on the other hand, to ensure air flow to help cooling the components.

The seven different phases as listed in Table 7 were combined and programmed into the test bench controller. The complete sequence becomes apparent from the diagrams and graphs in Fig. 28, Fig. 29, and Fig. 30.

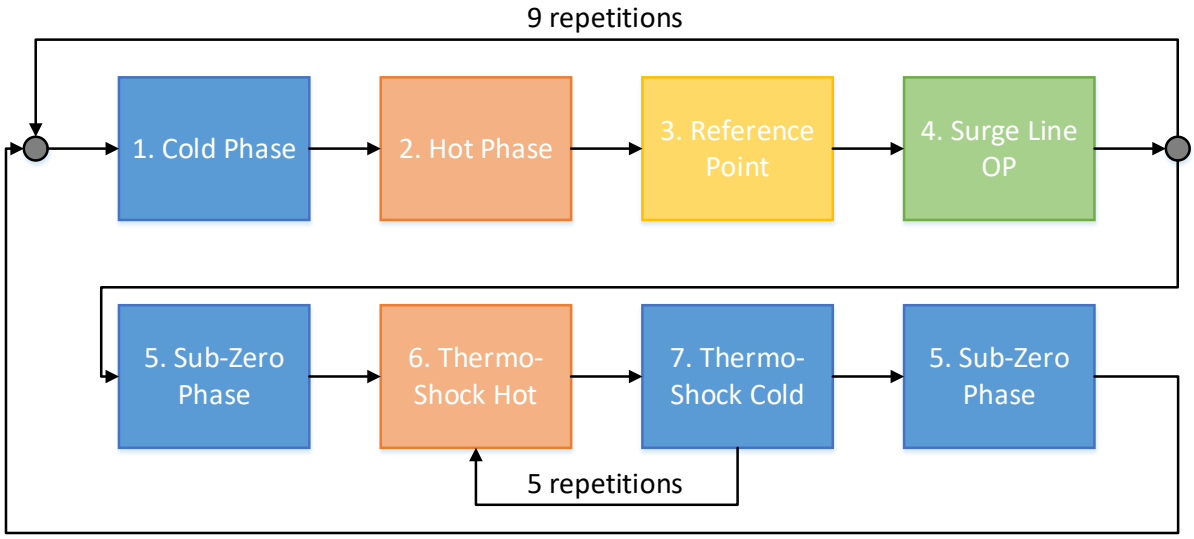

Fig. 28: Test bench flow control

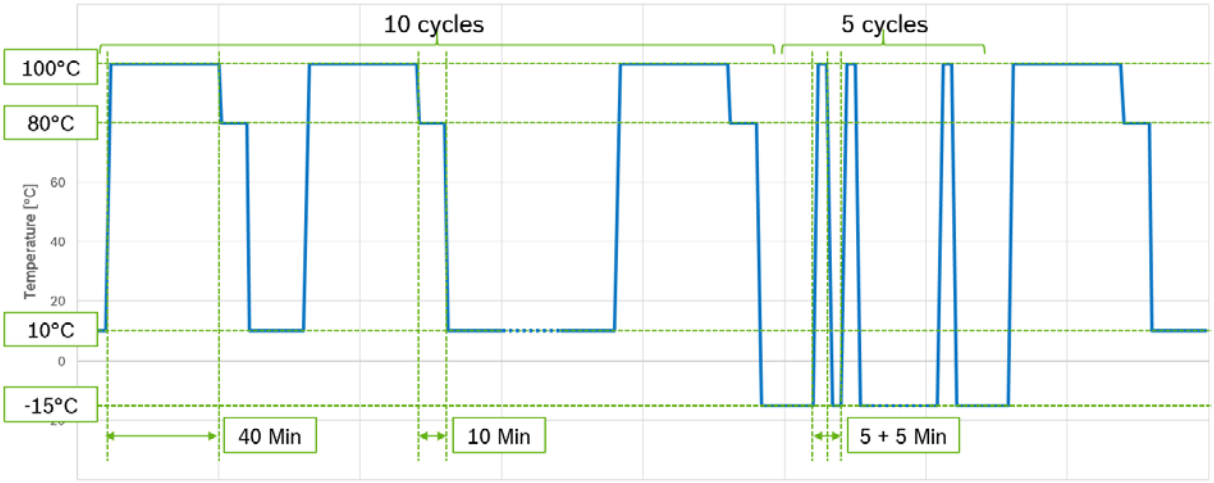

Fig. 29: Temperature desired values for test cycle

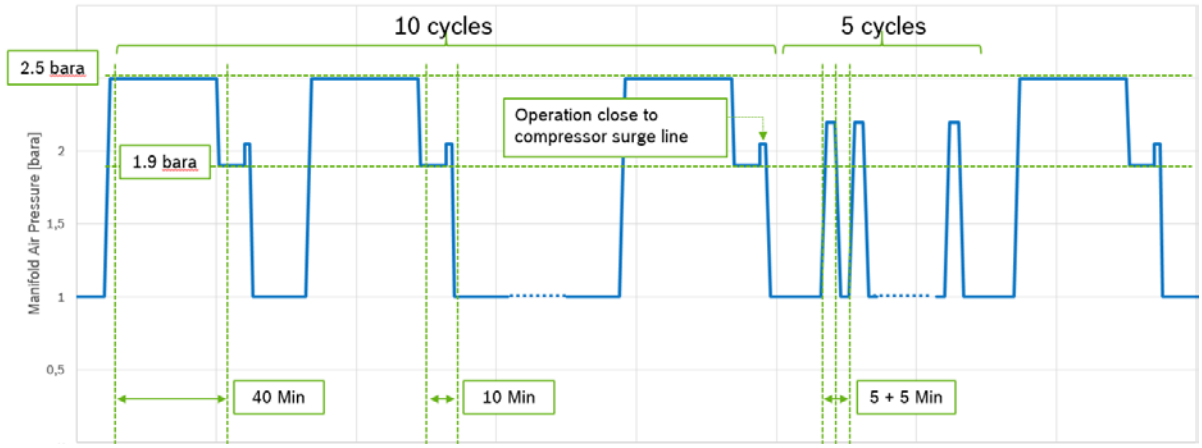

Fig. 30: Pressure desired values for test cycle

The temperature change in the interior of the humidifier is relatively slow in reaction to changes in intake air temperature and highly depends on the position. During set-up we implemented a logic circuit that stops cooling at 0 °C for the cold phase and -20 °C for the sub-zero phase in order to prevent damage due to overstrain. Fig. 31 shows a measured temperature profile for the different phases. The graph drawn in Fig. 32 proves that pressure response is almost instant.

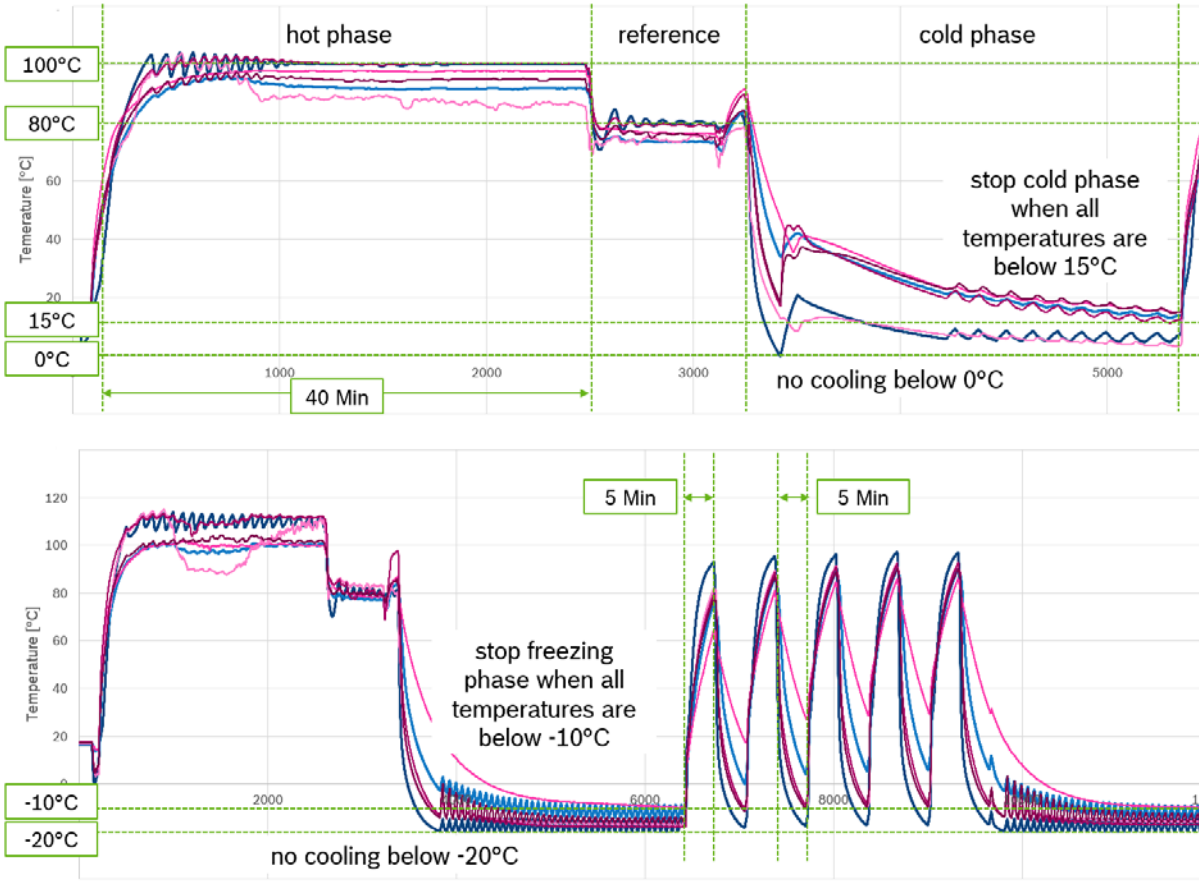

Fig. 31: Measured temperature profiles

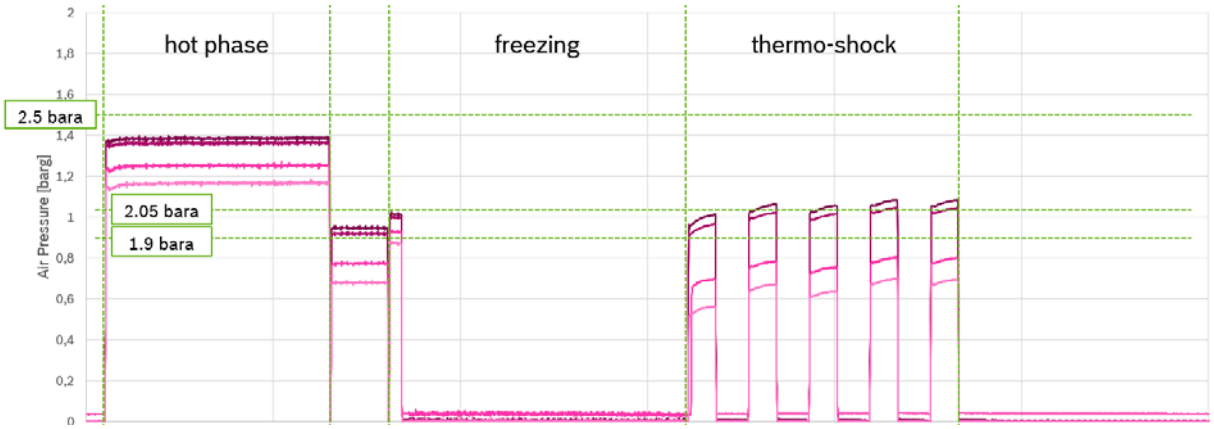

Fig. 32: Measured pressure profiles

6 Test results

6.1 Failure of components

6.1.1 Compressor

Focus of WP5.3 was the evaluation of performance losses over lifetime. Nevertheless during testing also total failure of various components occurred.

When we received the compressor used for disassembly and analysis of the components, we noticed that it had been dropped during transport. Besides mechanical damage to the housing and low voltage connectors, transmission fluid had leaked through the sealing into the air path. Further investigation showed that, under adverse conditions during compressor standstill, leakage of oil into the air system is possible. Since oil contamination will cause irreversible damage to the fuel cell and humidifier membranes, Rotrex compressors seem not to be the ideal solution for fuel cell air supply. Other systems making use of Rotrex components suggest that a deployment is still possible under careful attention to mounting and maintenance instructions. Growing demand presumably will bring forward other technology to ensure oil-free air supply.

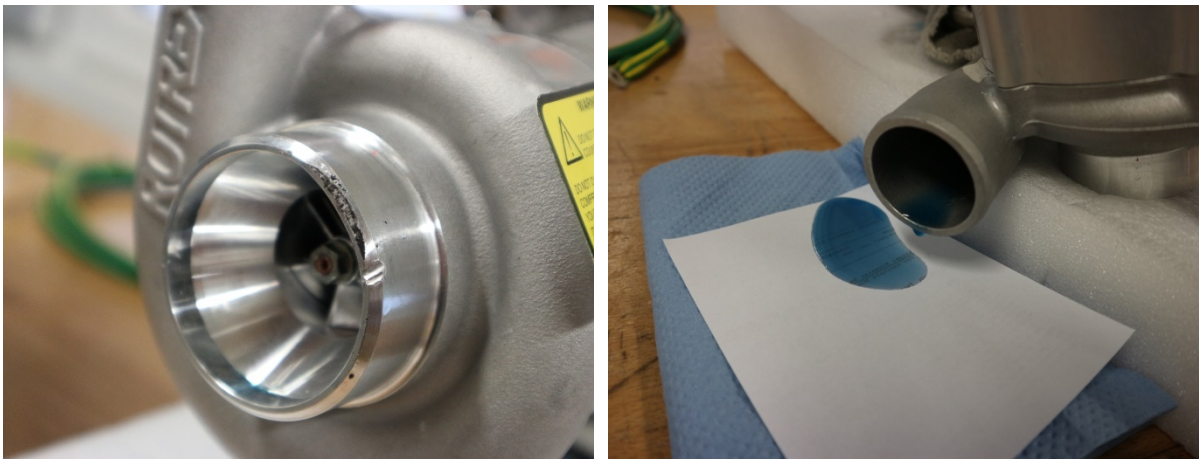

Fig. 33: Shipping damage of Rotrex compressor and oil spill

The first compressor unit used on the test bench failed with a broken impeller shaft after about 200 hours of use (endurance testing cycle 13). Examination of the failure revealed two decussate lubrication holes that act as a predetermined breaking point for the shaft, causing the impeller to crash into the volute housing. Other than aluminum chippings, again oil was able to enter the air path.

Fig. 34: Compressor failure due to broken impeller shaft

No metallic debris and no oil residue were found in the humidifier, so the testing could continue with a replacement compressor head unit. The measurement data though did unveil an operation point critically close to the surge line for the hot phase, which had not been detected during the installment of the test cycle. Consequently, the backpressure of the fuel cell simulation was reduced slightly, so that the replacement unit completed the test run for another 320 hours without any problems.

Fig. 35 displays the operation points of four exemplary test cycles in the Rotrex EC15-20 compressor map. Next to the intended operation close to the surge line for phase four of the test cycle (blue circle) and some very few transients, the orange and yellow COP show, that especially during hot phase the compressor is run very close to the surge line for a very long time (red circle). By reducing the back pressure after the first failure, the OP was moved more to the center of the flow map (green circle).

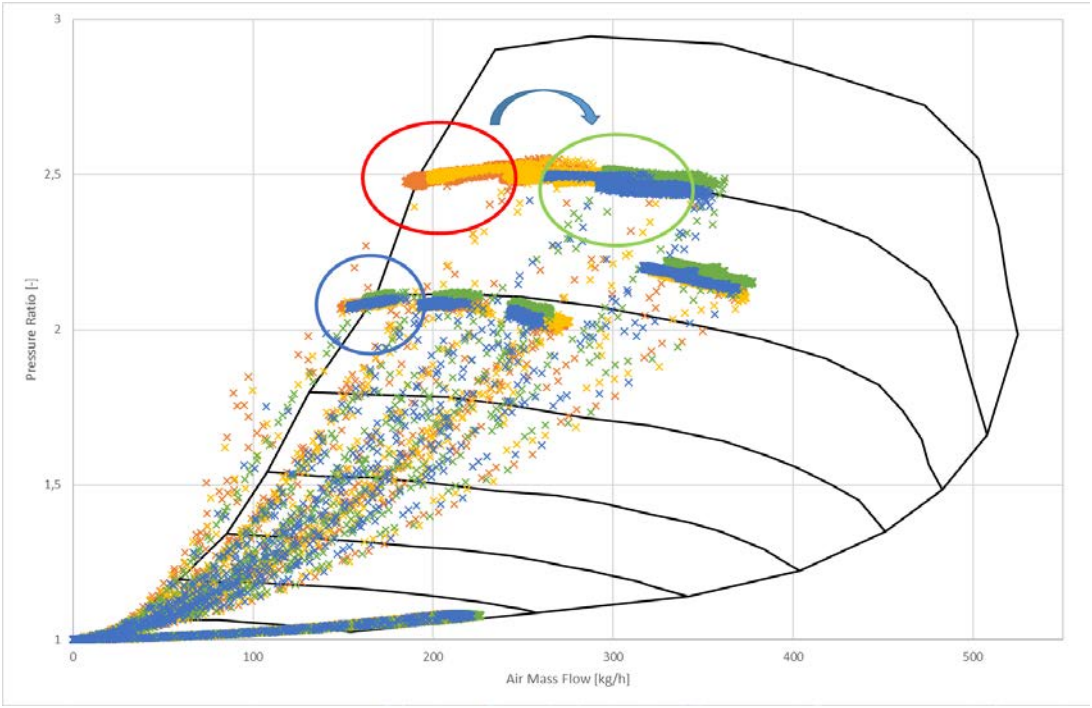

Fig. 35: Operating points in compressor map

Evaluation of the measured data gives no hint of how this failure could have been prevented other than a clean calibration of the operating points before. Even the readings of the vibration and Spike Energy measurements only gave suspicious values when the failure was already imminent.

The total value of the Spike Energy parameter is very much dependent on the mounting situation of the vibration sensor, so the information is in the changes. Fig. 36 shows, that only two cycles, or about three hours, before the emergency stop occurred, a significant change in the gSE signal could have been noticed.

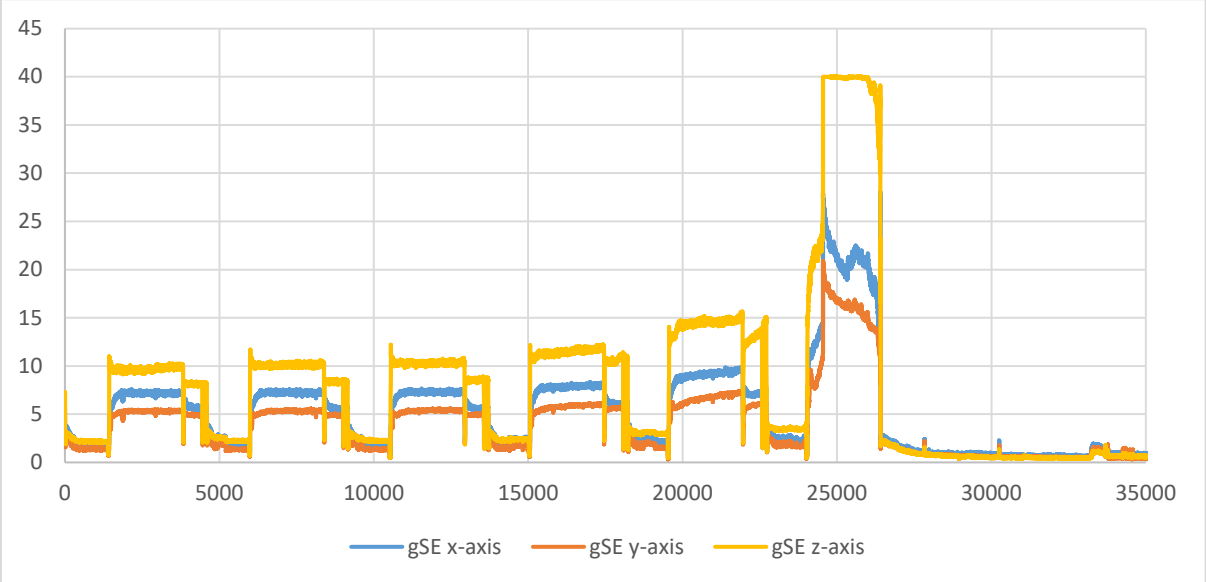

Fig. 36: Readings of Spike Energy measurement

6.1.2 Humidifier

In the first set-up of the test bench, the cables for the thermo-couples HUM_005, HUM_009, HUM_012, and HUM_015 inside the fiber bundles were run through holes drilled into the inlet end cover. Very soon, still during calibration of the test bench, this end cover broke and was blown off during a high temperature, high pressure phase (Fig. 37). The cover then was replaced and the cables were run a different route through the intake porthole. Shortly afterwards, the second end cover was blown off as well (Fig. 37). Examination of the parts and consultation with Fumatech showed that in the prototypes used the necessary amount of glass fibers was missing in the molded plastic. After replacing both covers with production parts, no problems occurred until the end of the test run.

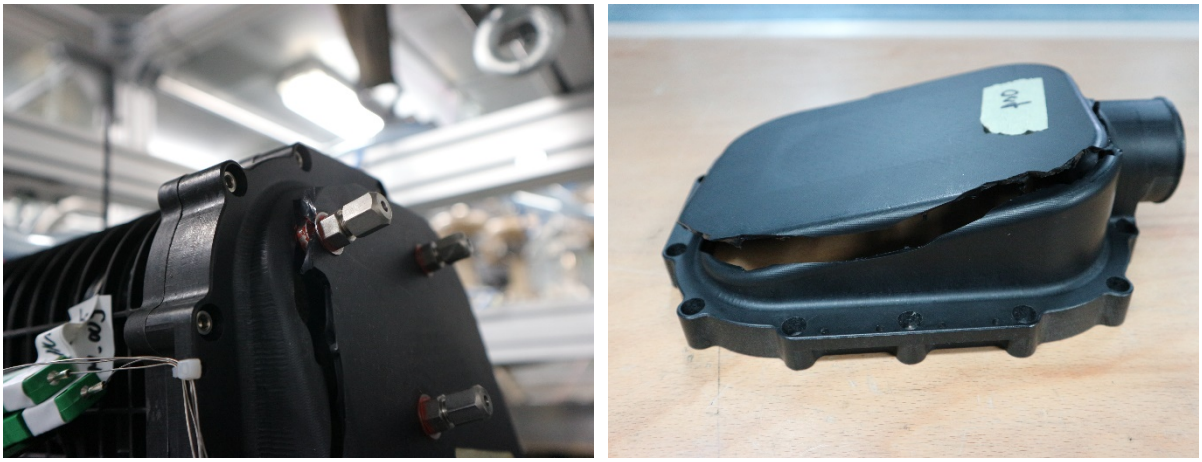

Fig. 37: Broken end covers of the humidifier

For the simulation of the fuel cell stack and source of humidity, the test bench deployed an electric heater combined with a dosing unit for liquid water. When a relay for the actuation of a water valve failed, hot and dry air of about 250°C was admitted to the humidifier port HUM3, causing burning of the fibers and melting of the shell housing (Fig. 38). Since this happened at a very early stage, the component was replaced and the whole test run re-started from the beginning.

Fig. 38: Humidifier destroyed by over-temperature

6.2 Evaluation of measurement data

All measurement data files are available on the Giantleap e-room server for further evaluation. A complete list of the data available can be found in Appendix B: Measurement data available on Giantleap e-room.

After uploading the data, we held a Skype meeting between UFC (Nadia Steiner, Raffaele Petrone) and BEG (Peter Eckert) to clarify open questions since the bulk of the evaluation was done by UFC.

6.2.1 Compressor

The main value to show performance losses of the compressor during lifetime is its efficiency. To calculate the efficiency, the thermal work of the compressor is compared to the electrical power consumed:

$$\mu_{COM} = \frac{P_{COM}}{P_{DC}} = \frac{\dot{m}_{COM} \cdot c_{p,COM} \cdot \left(T_{COM\_2} - T_{COM\_1}\right)}{U_{DC} \cdot I_{DC}}$$

In about 200 reference cycles or about 320 hours endurance testing, about 0.5 % of the efficiency is lost. In Fig. 39 the efficiency of the compressor is displayed. After reference-cycle 125 a new compressor was used because of the damage described above. Also the operating point for the hot phase was changed. Based on the measurement data of the new compressor, a linear regression was calculated using a non-linear least square fit and an exponential function

$$y = a \cdot e^{b \cdot x} + c$$

with the parameters a = 1.7009, b = -0.0016, and c = 80.0931.

The result is shown in Fig. 39. Because of the wide scatter of the measured values, the coefficient of determination R^2 = 0.073 is rather low.

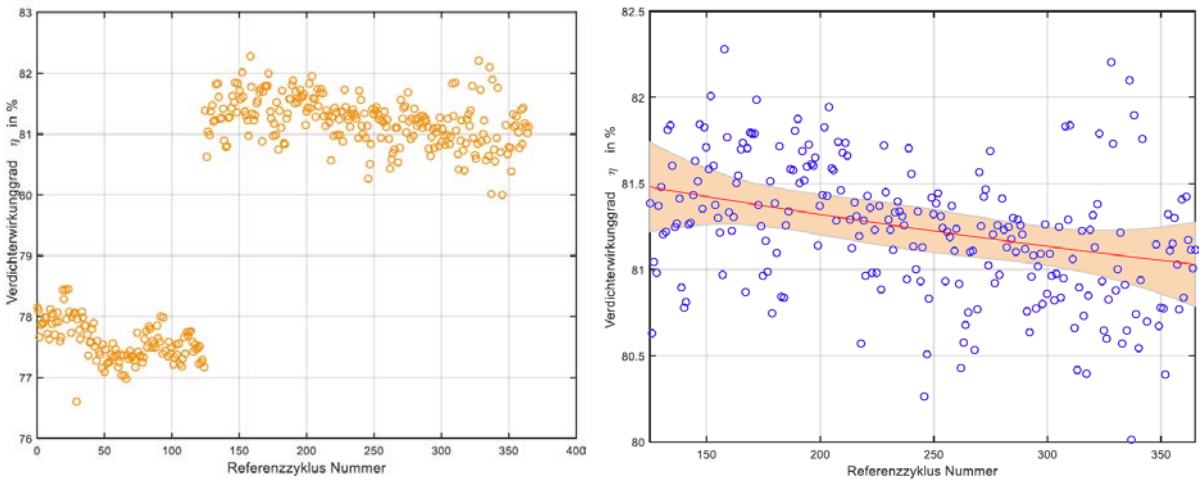

Fig. 39: Compressor efficiency, raw data and linear fit

6.2.2 Humidifier

One of the main observation concerning the humidifier is a rather low calculated efficiency of about 15%. Main reason is the high desired air temperature of about 100 °C, resulting in a very high capacity of the air to take on water. So, for a desired 95 % RH to be reached, the available heater and water

vaporizing capacity of the fuel cell stack simulation is way too low in power. So, the relative humidity at humidifier port HUM_3 remains at a quite low value.

For the calculation of the humidifier efficiency, the mass flow of water transported through the membranes $\dot{m}_{H_2O}$ is calculated from the air mass flow, pressure and temperature conditions, measured RH and amount of water injected into the system. From this the efficiency is calculated as

$$\mu_{HUM} = \frac{\dot{m}_{H_2O,HUM2} - \dot{m}_{H_2O,HUM1}}{\dot{m}_{H_2O,HUM3}}$$

Fig. 40 shows the resulting values. The step visible after about 200 reference cycles is due to some changes in the test bench set-up and was compensated for the linear regression.

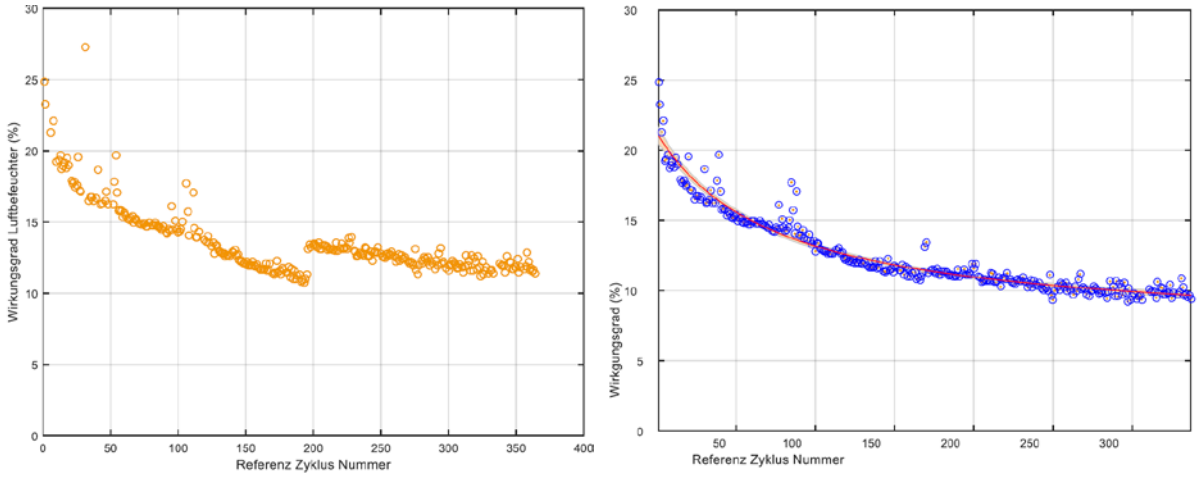

Fig. 40: Humidifier efficiency, raw data and linear fit

For the linear regression an exponential function of the form

$$y = \frac{a \cdot x + b}{x + c}$$

was used with the parameters a = 7.1084, b = 1601, and c = 75.3594. For the humidifier the coefficient of determination R^2 = 0.944 gives a very good fit.

From the measurements arises the assumption that the humidifier will lose about half of its efficiency in the beginning of its life and then stabilize at about 50 % of the original value.

After the endurance run, the fibers were screened for oil residue, but none was found.

7 Conclusion and Prospects

The test series did show that, with the components selected for the air path, a fuel cell system can operate for a period long enough for demonstration purposes. For this to be achieved, the operation strategy has to be fine-tuned to not destroy components by running them out of specification.

For the compressor, further development has to make sure that the air delivered to the fuel cell is free of oil under any circumstances. More development work also has to be spend to reduce size und improve durability for lifetime demands of commercial vehicles. As this report shows, for the compressor a degradation over lifetime will be marginal and a rest of useful lifetime will be difficult to define, because catastrophic failure is likely to dominate over continuous performance losses.

The humidifier did suffer a considerable amount of performance loss during this test run. Other measurements conducted by BEG on the systems test bench prove that a new Ecomate H50 humidifier is highly sufficient for the Giantleap fuel cell system. The test specimen however lost about half of its performance during the test run. Further development and testing will have to verify those numbers, but this behavior has to be kept in mind for the dimensioning of future systems.

The demand for fuel systems as power supply for electrically driven buses and other commercial vehicles is growing. Still, balance-of-plant components are not yet readily available on the market. Therefore, when the fuel cell system for the Giantleap project was designed, the requirement for the best components possible for the task had to step back behind availability of components on the market. Current developments however make it probable that some of the issues faced by the Giantleap system will be solved in the next generation.

8 Figure and Table Overview

9 Table of Abbreviations

BEG	Bosch Engineering GmbH
BoP	Balance of Plant
CAD	Computer Aided Design
COP	Cloud of Points
D	Deliverable
DC/DC	Direct current to direct current
DIN	German Institute for Standardization (Deutsches Institut für Normung)
DSC	Differential scanning calorimetry
EK	ElringKlinger
EN	European standard (Europäische Norm)
e-bus	Electric bus
ECU	Electronic control unit
E/E	Electric and Electronic
FC	Fuel Cell
FCCU	Fuel Cell Control Unit
HV	High Voltage
HGI	Hydrogen Gas Injector
InvCon	Integrated Inverter and Converter
LV	Low Voltage
MEA	Membrane electrolyte assembly
NOW	German national organization for hydrogen and fuel cells (Nationale Organisation Wasserstoff- und Brennstoffzellentechnologie)
OP	Operation piont
PEM	Proton exchange membrane
PWM	Pulse Width Modulation
P&ID	Piping and Instrumentation Diagram
REEV	Range Extended Electric Vehicle
RH	Relative Humidity
SMG	Separate motor generator
TGA	Thermo-gravimetric analysis
Temp.	Temperature
UFC	Université de Franche-Comté
VCU	Vehicle Control Unit
VDI	Association of German Engineers (Verein Deutscher Ingenieure)
WP	Work Package

10 Literature

1. *GiantLeap Improves Automation of Non-polluting Transportation with Lifetime Extension of Automotive PEM fuel cells.* **2015, FCH2 JU Call for Proposals.** Brussels : s.n., August 2015. H2020-JTI-FCH-2015-1.

2. **Belschner, Werner.** *Fuel Cell System Design.* Abstatt : Bosch Engineering GmbH, May 2017. GiantLeap Deliverable D5.2.

3. **Jung, Heiko, et al.** *Wasserstoffdosierventil für die Anodengasversorgung von Kfz-Brennstoffzellensystemen, Hydrogen Gas Injector (HGI).* Schwieberdingen : Robert Bosch GmbH, December 2013. Final Report.

4. **Rotrex.** *Technical Data Sheet C15 Supercharger Range.* www.rotrex.com : s.n. Version 5.0.

5. —. *Rotrex C-range Superchargers - Setup and Maintenance.* Version 9.1.

6. —. *Rotrex Technical Handbook.* www.rotrex.com : s.n. Version 1.1.

7. **Aldi, Nicola, et al.** An Interdisciplinary Approach to Study the Fouling Phenomenon. *Energy Procedia.* 2015, 82.

8. **Suman, Alessio, et al.** A Compressor Fouling Review Based on an Historical Survey of ASME Turbo Expo Papers. *Journal of Turbomachinery.* 2017, 139.

9. **Balan, C. und Tabakoff, W.** Axial flow compressor performance deterioration. *AIAA-Papers.* 1984.

10. *Damage Analysis of Automotive Turbo Chargers.* **Lozanovic Sajic, Jasmina und Lozanovic, Veljko.** Chemnitz : MEKO TC15 - Experimental Mechanics - 10th YSESM, 2011.

11. **Manson, S. S., et al.** *Factors Affecting Vibration of Axial Flow Compressor Blades.* Cleveland, Ohio : National Commitee for Aeronautics.

12. **Mathuria, P. H., et al.** Vibration and Shock Considerations in the Design of a Truck-mounted Fuel Cell APU System. *SAE Transactions.* Journal of Commercial Vehicles, 2002, 111.

13. **Rao, Rama und Dutta, B. K.** Vibration analysis for detecting failure of compressor blade. *Engineering Failure Analysis.* 2012, 25.

14. **Ren, Tianming und Feng, Ming.** Anti-Shock Characteristics of Water Lubricated Bearing for Fuel Cell Vehicle Air Compressor. *Tribology International.* 2016, 107.

15. **Asciano, G. M. und Wang, Weiji.** *Diesel Engine Turbocharger Performance Monitoring Using Vibration Analysis.* University of Sussex, UK : SAE Technical Paper Series, 2007.

16. **Zhao, Dongdong.** *Control of an ultrahigh speed centrifugal compressor for.* Belfort, France : University of Technology of Belfort-Montbeliard, 2014.

17. **Luo, Shuai und Wu, Sujun.** *Fatigue failure analysis of rotor compressor blades concerning the effect of rotating stall and surge.* Beijing : Elsevier Science, 2016. 1350-6307.

18. **Cho, Han-Wook, et al.** *Rotor Natural Frequency in High-Speed Permanent-Magnet Synchronous Motor for Turbo-Compressor Application.* Daejon, Korea : IEEE Transactions on Magnetics, 2011.

19. **Filipczyk, Jan.** *Causes of Automotive Turboscharger Faults.* Katowice, Poland : Silesian University of Technology, Faculty of Transport, 2013.

20. **Mahle.** *Turbocharger: Damage Profiles, Causes, and Prevention.* Ann Arbor, Michigan : Mahle Aftermarket. MO-2-612.

21. *Gas Turbine Degradation.* **Kurz, Rainer, Meher-Homji, Cyrus und Brun, Klaus.** Huston, Texas : 43rd Turbomachinery & 30th Pump Users Symposia (Pump & Turbo 2014), 2014.

22. **Izidor, Marek, Karpiuk, Wojciech und Bieliński, Maciej.** Operating Problems of Turbocharging Systems in Compression-Ignition Engines. *Journal of Polish Cimac.*

23. **Lee, Adrian P.** Full-Toroidal Traction Drive Variator Material and Fluid Durability. *SAE International Journal of Engines.* 2011, Bd. 1, 4.

24. **Rotomaster.** *Turbocharger Warranty - Analysis Guidelines.* [https://www.vividracing.com/productdocs/Rotomaster_Turbocharger_Information.pdf] Surrey, Canada : Rotomaster.

25. **McCraig, M. S., Paul, D. R. und Barlow, J. W.** Effect of film thickness on the changes in gas permeability of a glassy polyarylate due to physical ageing Part II. Mathematical model. *Polymer.* 2, 2000, 41.

26. **Dr. Wieneke, Jan Ulrich.** *Thermische Alterung von 6FDA Polyimiden.* Düsseldorf : Heinrich Heine Universität Düsseldorf, 2009.

27. **Zhou, Chun, et al.** A governing equation for physical ageing of thick and thin fluoropolyimide films. *Journal of Applied Polymer Science.* 3, 2004, 92.

28. **Hu, Chien-Chieh, et al.** Effect of physical ageing on the gas transport properties of poly(methyl methacrylate) membranes. *Journal of Membrane Science.* 1-2, 2007, 303.

29. **DKE Deutsche Kommission Elektrotechnik Elektronik Informationstechnik im DIN und VDE.** Methods for product accelerated testing. Berlin, Germany : DIN Deutsches Institut für Normung e. V, 2013. DIN EN 62506.

30. **Wikipedia.** *Vortex tube.* [https://en.wikipedia.org/wiki/Vortex_tube]

31. **Xu, Ming.** *Spike Energy Measurement and Case Histories.* [Integrated Condition Monitoring] Westerville, Ohio, USA : Rockwell Automation.

11 Appendix

11.1 Appendix A: List of measuring points

Label	Unit	Description
SysDateTime		Measurement System Time Stamp [dd.mm.yyyy hh:mm:ss]
Zeit	s	Measurement Time
CV_BPU1_mv	%	Control Value Back Pressure Unit 1 (simulation pressure loss in fuel cell stack)
CV_BPU2_mv	%	Control Value Back Pressure Unit 2 (pressure regulation valve in exhaust system)
I_COM_0_mv	A	Current demand air compressor
I_EM_DC_mv	A	Current demand air compressor electric motor
I_HVQ_mv	A	Current output high voltage supply
Lvl_DRA_0_mv	%	Water level in drainage container of water injection system
M_COM_0_mv	Nm	Torque air compressor (from CAN)
M_EM_mv	Nm	Torque air compressor motor (from CAN)
NotAus		Status emergency stop
P_CON1_0_mv	kW	Power conditioning unit 1 (simulation heat source fuel cell stack)
P_HVQ_mv	W	Power output high voltage supply
T_A_mv,	°C	Air temperature of test bench compressed air supply
T_COM_1_mv	°C	Air temperature at air compressor intake
T_COM_2_mv	°C	Air temperature at air compressor outlet
T_CON1_2_mv	°C	Air temperature at outlet of condioning unit 1
T_EM_Rot_mv	°C	Rotor temperature of air compressor electric motor (from CAN, software model)
T_EM_cw_1_mv	°C	Cooling water temperature at intake of air compressor electric motor
T_EM_cw_2_mv	°C	Cooling water temperature at outlet of air compressor electric motor
T_EM_mv	°C	Temperature of air compressor electric motor (from CAN)
T_ENV_1_mv	°C	Ambient air temperature in test location
T_GEA_1_mv	°C	Oil temperature at air compressor drive intake
T_GEA_2_mv	°C	Oil temperature at air compressor drive outlet
T_GEA_cw_1_mv	°C	Cooling water temperature at air compressor drive oil cooler intake
T_GEA_cw_2_mv	°C	Cooling water temperature at air compressor drive oil cooler outlet
T_HUM_005_mv	°C	Temperature inside humidifier fibre bundle No. 5
T_HUM_009_mv	°C	Temperature inside humidifier fibre bundle No. 9
T_HUM_012_mv	°C	Temperature inside humidifier fibre bundle No. 12
T_HUM_015_mv	°C	Temperature inside humidifier fibre bundle No. 15
T_HUM_1_mv	°C	Air temperature at humidifier port 1 (intake fresh air)
T_HUM_1_rot_mv	°C	Air temperature at humidifier port 1 (intake fresh air)
T_HUM_2_mv	°C	Air temperature at humidifier port 2 (outlet humidified air)
T_HUM_2_rot_mv	°C	Air temperature at humidifier port 2 (outlet humidified air)
T_HUM_3_mv	°C	Air temperature at humidifier port 3 (intake wet air from fuel cell stack)
T_HUM_3_rot_mv	°C	Air temperature at humidifier port 3 (intake wet air from fuel cell stack)

Label	Unit	Description
T_HUM_4_mv	°C	Air temperature at humidifier port 4 (exhaust)
T_HUM_4_rot_mv	°C	Air temperature at humidifier port 4 (exhaust)
T_INC_cw_1_mv	°C	Cooling water temperature at charge air cooler (intercooler) intake
T_INC_cw_2_mv	°C	Cooling water temperature at charge air cooler (intercooler) outlet
T_INV_cw_1_mv	°C	Cooling water temperature at air compressor drive inverter intake
T_INV_cw_2_mv	°C	Cooling water temperature at air compressor drive inverter outlet
T_INV_cw_mv	°C	Cooling water temperature at air compressor drive inverter (from CAN)
T_INV_mv	°C	Component temperature air compressor drive inverter (from CAN)
U_COM_0_mv	V	Supply voltage air compressor
U_EM_DC_mv	V	Supply voltage air compressor drive electric motor
U_HVQ_mv	V	Supply voltage high voltage supply
Vdot_DRA_0_mv	m3/h	Water volume flow in drain unit (simulation air humidification by fuel cell stack)
Vdot_WCU_2_mv	l/min	Water volume flow through water conditioning unit 2 (water conditioning for charge air cooler)
cold_counter	s	Duration of current cooling cycle
cycle_HT		Cycle counter: Number of high temperature cycles (current run)
cycle_TS		Cycle counter: Number of thermal shock cycles (current run)
cycle_TS_cold		Cycle counter: Number of thermal shock high temperature cycles (total)
cycle_TS_hot		Cycle counter: Number of thermal shock low temperature cycles (total)
cycle_cold		Cycle counter: Number of cool temperature cycles (total)
cycle_freeze		Cycle counter: Number of cold temperature / freezing cycles (total)
cycle_hot		Cycle counter: Number of high temperature cycles (total)
cycle_ref		Cycle counter: Number of reference point cycles (total)
cycle_surge		Cycle counter: Number of cycles with operation point near air compressor surge line (total)
disp_counter		Duration of current cycle
dp_COM_1_mv	bar	Realtive air pressure at air compressor intake
dp_COM_2_mv	bar	Relative air pressure at air compressor outlet
dp_GEA_2_mv	bar	Relative oil pressure at oil pump outlet
dp_HUM_1_mv	bar	Relative air pressure at humidifier port 1 (intake fresh air)
dp_HUM_2_mv	bar	Relative air pressure at humidifier port 2 (outlet humidified air)
dp_HUM_3_mv	bar	Relative air pressure at humidifier port 3 (intake wet air from fuel cell stack)
dp_HUM_4_mv	bar	Relative air pressure at humidifier port 4 (exhaust)
dp_INJ_1_mv	bar	Relative water pressure at water injector (simulation air humidification by fuel cell stack)
dp_WCU_2	bar	Relative water pressure at water conditioning unit 2 (water conditioning for charge air cooler)
freeze_counter	s	Duration of current freezing cycle
gSE_COM_x_mv	gSE	Air compressor bearing condition monitoring, load value x axis
gSE_COM_x_mv_2s	gSE	Air compressor bearing condition monitoring, load value x axis

Label	Unit	Description
gSE_COM_y_mv	gSE	Air compressor bearing condition monitoring, load value y axis
gSE_COM_y_mv_2s	gSE	Air compressor bearing condition monitoring, load value y axis
gSE_COM_z_mv	gSE	Air compressor bearing condition monitoring, load value z axis
gSE_COM_z_mv_2s	gSE	Air compressor bearing condition monitoring, load value z axis
m_dot_A_mv,	kg/h	Air mass flow of test bench compressed air supply (for vortex cooling pipes)
mdot_COM_1_mv	kg/h	Air mass flow through air compressor
mdot_DRA_mv	kg/h	Water mass flow in drain unit (simulation air humidification by fuel cell stack)
mdot_GEA_1_mv	kg/h	Oil mass flow through air compressor drive oil system
mdot_INJ_0_mv	kg/h	Water mass flow though water injector (simulation air humidification by fuel cell stack)
mdot_w_HUM_1_mv	kg/h	Water mass flow at humidifier port 1 (intake fresh air)
mdot_w_HUM_2_mv	kg/h	Water mass flow at humidifier port 2 (outlet humidified air)
mdot_w_HUM_3_mv	kg/h	Water mass flow at humidifier port 3 (intake wet air from fuel cell stack)
mdot_w_HUM_mv	kg/h	Water mass flow at humidifier port 4 (exhaust)
n_COM_0_mv	rpm	Speed of air compressor impeller
n_EM_mv	1/min	Speed of air compressor electroc motor
p_ENV_1_mv	bar	Ambient air pressure in test location
p_diff_GEA_1_2_mv	bar	Differential oil pressure by air compressor drive oil pump
rh_COM_1_mv	%	Relative humidity at air compressor intake
rh_ENV_1_mv	%	Relative humidity of ambient air in test location
rh_HUM_1_mv	%	Relative humidity at humidifier port 1 (intake fresh air)
rh_HUM_2_mv	%	Relative humidity at humidifier port 2 (outlet humidified air)
rh_HUM_3_mv	%	Relative humidity at humidifier port 3 (intake wet air from fuel cell stack)
rh_HUM_4_mv	%	Relative humidity at humidifier port 4 (exhaust)
rho_INJ_0_mv	kg/m³	Water density at water injector (simulation air humidification by fuel cell stack)
seq_sts		Sequence status of test automation
v_COM_x_mv	mm/s	Vibration sensor speed, x axis
v_COM_x_mv_2s	mm/s	Vibration sensor speed, x axis
v_COM_y_mv	mm/s	Vibration sensor speed, y axis
v_COM_y_mv_2s	mm/s	Vibration sensor speed, y axis
v_COM_z_mv	mm/s	Vibration sensor speed, z axis
v_COM_z_mv_2s	mm/s	Vibration sensor speed, z axis
eta_HUM	%	Calculated humidifier efficiency

11.2 Appendix B: Measurement data available on Giantleap e-room

Name	Date modified		Type	Size
BoP_Ageing_Measurement_ Meta-Data.xlsx	28.06.2018	15:22	Microsoft Excel Worksheet	578,873 KB
Dauerlauf_Zyklus_01_1Hz.xlsx	02.05.2018	07:27	Microsoft Excel Worksheet	61,854,406 KB

Name	Date modified		Type	Size
Dauerlauf_Zyklus_02_1Hz.xlsx	02.05.2018	07:31	Microsoft Excel Worksheet	76,310,608 KB
Dauerlauf_Zyklus_03_1Hz.xlsx	02.05.2018	07:35	Microsoft Excel Worksheet	68,985,662 KB
Dauerlauf_Zyklus_04_1Hz.xlsx	02.05.2018	07:39	Microsoft Excel Worksheet	69,820,361 KB
Dauerlauf_Zyklus_05_1Hz.xlsx	02.05.2018	07:43	Microsoft Excel Worksheet	65,590,486 KB
Dauerlauf_Zyklus_06_1Hz.xlsx	02.05.2018	07:46	Microsoft Excel Worksheet	63,552,400 KB
Dauerlauf_Zyklus_07_1Hz.xlsx	02.05.2018	07:49	Microsoft Excel Worksheet	63,917,191 KB
Dauerlauf_Zyklus_08_1Hz.xlsx	03.05.2018	14:30	Microsoft Excel Worksheet	63,977,492 KB
Dauerlauf_Zyklus_09_1Hz.xlsx	03.05.2018	12:18	Microsoft Excel Worksheet	63,977,492 KB
Dauerlauf_Zyklus_10_1Hz.xlsx	04.05.2018	10:46	Microsoft Excel Worksheet	63,600,025 KB
Dauerlauf_Zyklus_11_1Hz.xlsx	04.05.2018	10:36	Microsoft Excel Worksheet	62,746,718 KB
Dauerlauf_Zyklus_12_1Hz.xlsx	07.05.2018	08:38	Microsoft Excel Worksheet	64,573,369 KB
Dauerlauf_Zyklus_13_1Hz.xlsx	18.05.2018	05:44	Microsoft Excel Worksheet	101,307,606 KB
Dauerlauf_Zyklus_14_1Hz.xlsx	18.05.2018	14:17	Microsoft Excel Worksheet	67,894,256 KB
Dauerlauf_Zyklus_15_1Hz.xlsx	22.05.2018	05:04	Microsoft Excel Worksheet	62,753,741 KB
Dauerlauf_Zyklus_16_1Hz.xlsx	22.05.2018	05:08	Microsoft Excel Worksheet	64,632,342 KB
Dauerlauf_Zyklus_17_1Hz.xlsx	22.05.2018	05:12	Microsoft Excel Worksheet	66,608,542 KB
Dauerlauf_Zyklus_18_1Hz.xlsx	22.05.2018	05:33	Microsoft Excel Worksheet	70,809,137 KB
Dauerlauf_Zyklus_19_1Hz.xlsx	22.05.2018	05:49	Microsoft Excel Worksheet	69,704,648 KB
Dauerlauf_Zyklus_20_1Hz.xlsx	23.05.2018	06:58	Microsoft Excel Worksheet	63,558,593 KB
Dauerlauf_Zyklus_21_1Hz.xlsx	23.05.2018	09:59	Microsoft Excel Worksheet	62,075,455 KB
Dauerlauf_Zyklus_22_1Hz.xlsx	24.05.2018	06:09	Microsoft Excel Worksheet	64,050,521 KB
Dauerlauf_Zyklus_23_1Hz.xlsx	25.05.2018	06:38	Microsoft Excel Worksheet	71,373,693 KB
Dauerlauf_Zyklus_24_1Hz.xlsx	25.05.2018	06:25	Microsoft Excel Worksheet	62,686,924 KB
Dauerlauf_Zyklus_25_1Hz.xlsx	28.05.2018	05:26	Microsoft Excel Worksheet	67,956,935 KB
Dauerlauf_Zyklus_26_1Hz.xlsx	28.05.2018	05:29	Microsoft Excel Worksheet	65,891,962 KB
Dauerlauf_Zyklus_27_1Hz.xlsx	28.05.2018	05:33	Microsoft Excel Worksheet	65,417,345 KB
Dauerlauf_Zyklus_28_1Hz.xlsx	28.05.2018	05:38	Microsoft Excel Worksheet	72,163,457 KB
Dauerlauf_Zyklus_29_1Hz.xlsx	28.05.2018	14:20	Microsoft Excel Worksheet	66,891,988 KB
Dauerlauf_Zyklus_30_1Hz.xlsx	30.05.2018	07:59	Microsoft Excel Worksheet	68,987,134 KB
Dauerlauf_Zyklus_31_1Hz.xlsx	30.05.2018	08:03	Microsoft Excel Worksheet	67,379,737 KB
Dauerlauf_Zyklus_32_1Hz.xlsx	30.05.2018	08:07	Microsoft Excel Worksheet	62,682,112 KB
Dauerlauf_Zyklus_33_1Hz.xlsx	04.06.2018	06:31	Microsoft Excel Worksheet	70,209,331 KB
Dauerlauf_Zyklus_34_1Hz.xlsx	12.06.2018	09:37	Microsoft Excel Worksheet	121,561,868 KB
Dauerlauf_Zyklus_35_1Hz.xlsx	12.06.2018	12:30	Microsoft Excel Worksheet	118,865,186 KB
Dauerlauf_Zyklus_36_1Hz.xlsx	06.06.2018	10:28	Microsoft Excel Worksheet	84,846,758 KB
Dauerlauf_Zyklus_37_1Hz.xlsx	07.06.2018	06:23	Microsoft Excel Worksheet	64,213,947 KB
Dauerlauf_Zyklus_38_1Hz_ unvollstaendig.xlsx	07.06.2018	06:24	Microsoft Excel Worksheet	7,987,625 KB